UNIVERSITY of CALIFORNIA
SANTA CRUZ

INVESTIGATION OF HOW ANGLE OF ATTACK AFFECTS ROTOR SPEED IN WIND TURBINES

A thesis submitted in partial satisfaction of the
requirements for the degree of

BACHELOR OF SCIENCE

in

APPLIED PHYSICS

by

Geno Thomas Viscuso

June 2011

The thesis of Geno Thomas Viscuso is approved by:

Professor Fred Kuttner Advisor	Professor David P. Belanger Senior Theses Coordinator

Professor David P. Belanger
Chair, Department of Physics

Abstract

A small wind turbine designed with variable-pitch blades is tested in UCSC's wind tunnel. The turbine is used to test how varying the blade angle affects the turbine's rotational speed at different wind speeds. The data are used to determine how the blade angle must change with wind speed to maintain a constant turbine rotational speed. Pitch control is confirmed as a means to control rotational speed for a wide range of wind speeds. Then the efficiency difference between variable speed operation and fixed speed operation is investigated. Variable speed operation is found to be more efficient than fixed speed operation over the majority of the tested wind speed range.

Acknowledgements

I would like to thank Bob Land and Rob Land for their help with designing the wind turbine and for their work machining parts. I would also like to thank Karen Groppi for teaching me AutoCAD and drafting practices. Finally, I would like to thank Professors Fred Kuttner and Dave Belanger for allowing me to research this topic, and thanks to my family for providing the necessary pressure and support.

Contents

1

Introduction

1.1 Wind Power

To determine the available power in the wind consider a thin disc of cross-sectional area A and thickness dx with incident wind at a speed w. The volume of wind passing through this disc at any time t is

$$dV = A\,dx\,.$$

This volume has a mass

$$dm = \rho_{air} A\,dx$$

where ρ_{air} is the density of air.

This mass, traveling at a speed w, has a kinetic energy

$$T = \frac{1}{2}\,mw^2 = \frac{1}{2}\,w^2 \rho_{air} A\,dx\,.$$

Power equals the time derivative of kinetic energy, so the available power in the disc is

$$\text{Power} = \frac{1}{2}\,w^2 \rho_{air} A \frac{dx}{dt} = \frac{1}{2}\,\rho_{air} A w^3\,. \qquad (1.1)$$

Thus wind power is proportional to the cube of the wind speed [1].

This relationship makes researching methods for harnessing wind power relevant.

1.2 Wind Turbines

1.2.1 Wind Turbine Basic Function and Structure

Different wind turbines can vary in design but all do one thing: convert kinetic energy from moving air into electricity [2]. Wind causes a torque on the turbine's blades and the resulting rotation drives a generator.

Most turbines are classified by the orientation of their axis of rotation: horizontal or vertical (see Fig. 1.1 for a typical picture of both turbine designs).

Horizontal axis wind turbines (HAWTs) are characterized by a horizontal main shaft. There are typically three blades that extend from the rotor hub and form a plane that, with the help of a yaw motor, faces into incoming wind. The rotor connects directly to a horizontal low-speed shaft. Wind forces create a torque on the rotor and cause the low-speed shaft to rotate. This shaft feeds into a 2- or 3-stage

Figure 1.1: Typical turbine designs. The horizontal-axis design [3] is on the left and the vertical-axis design [4] in on the right.

speed-increasing gearbox that turns a high-speed shaft [5]. Then the high-speed shaft feeds into the generator, thereby producing power. The shafts, gearbox, and generator are all housed in an aerodynamic structure called the nacelle. Figure 1.2 shows a cutaway of the nacelle for a typical HAWT. The nacelle and rotor are elevated above the ground via a tower to take advantage of the higher wind speeds (wind speeds increase with elevation due to the decrease in turbulence from objects on the ground). HAWTs must face into the wind to harness the maximum possible wind power, so they require an active yaw control system.

Vertical axis wind turbines (VAWTs) have a vertical main shaft. The blades are also vertical and have a plane of rotation perpendicular to that of a HAWT. Because the main shaft goes from the rotor to the ground, the gearbox and generator are

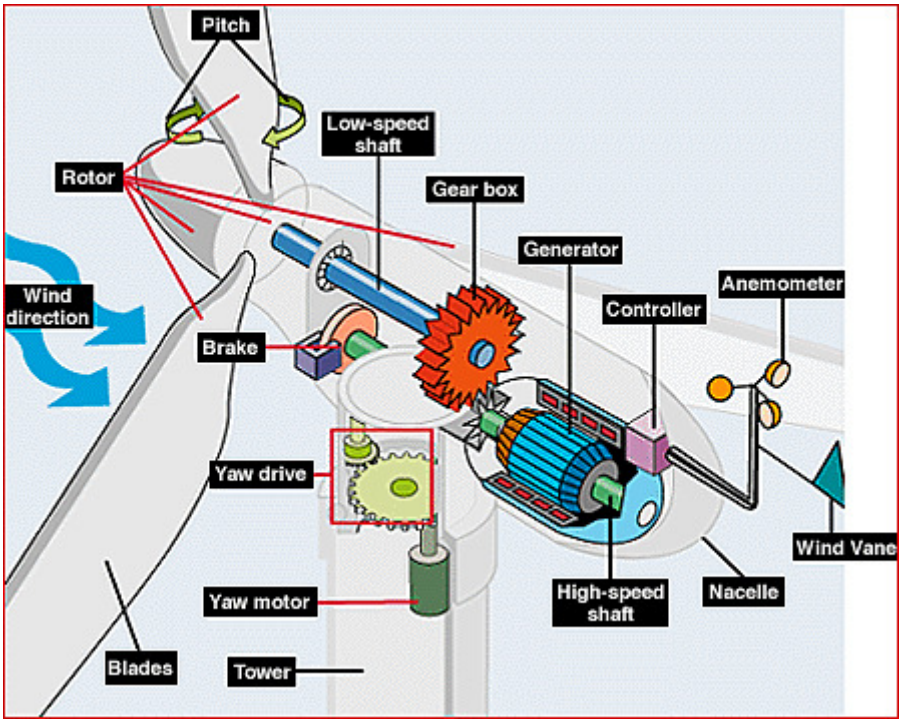

Figure 1.2: Cutaway of a typical HAWT [6].

housed on the ground, making maintenance easier than for a HAWT. However, VAWTs are less common in utility and residential applications because they are less efficient than HAWTs, so they are not a research interest in this paper.

1.2.2 Necessity and Methods for Regulating Rotational Speed

Turbines are designed to operate in a wide range of wind speeds, but are most efficient when operating in winds near their rated wind speed. A turbine with a fixed blade pitch, left unregulated, rotates at a slower speed under slower wind speeds and rotates much faster at wind speeds larger than the rated wind speed. Both cases are detrimental to power output if the turbine is directly connected to a power grid because the generator would produce power with a frequency and voltage that change with wind speed. This is not recommended because frequency and voltage fluctuations are harmful to any electrical equipment relying on steady input power.

To rectify this problem there exist several methods for regulating a turbine's output power: yaw control, mechanical and electrical braking, variable speed operation, stall control, and pitch control.

Increasing the yaw angle between the turbine axis and the incident wind results in a potential power falloff proportional to the cube of the cosine of the yaw angle (from equation 1.1 with $w = w_o \cos\lambda$ where λ is the yaw angle). Therefore increasing the yaw angle at high wind speeds will reduce the turbine's power output. However, it results in unequal forces acting on the rotor throughout its rotation. This causes the rotor to wobble and subjects it to greater fatigue [7].

Mechanical and electrical braking can also slow a turbine down when rotating too quickly. Turbines are equipped with disc or drum brakes to mechanically slow them down when operating above the rated rotational speed [8]. To electrically slow down a wind turbine, the generator is connected to a resistor bank; this increases the generator's impedance, so the extra torque from the wind turbine, instead of increasing the turbine's speed, is dissipated by the resistor bank as heat.

A method that reduces the amount of energy lost is to allow the turbine to rotate freely and then convert the generated power's variable frequency to that of the power grid via power-electronic converters [9]. With no energy being wasted to regulate the turbine, energy production is more efficient at a wider range of wind speeds compared to fixed-speed turbines [5]. Variable speed operation reduces mechanical stresses, improves output power quality, and reduces noise emission [2]. However, since some of the power generated must pass through a converter (which is not 100 percent efficient), some of the efficiency gain is lost in the conversion process [10].

Stall control involves pitching the turbine blades to a small angle. This decreases the torque acting to rotate the turbine such that at varying, high wind speeds the turbine's power output remains fairly constant [2].

Pitch control allows for reduced stress on the blades and can help regulate a turbine's rotational speed. Mechanical methods exist for controlling blade pitch for smaller-scale turbines, but power is required for pitch control systems in large-scale turbines due to the weight and amount of force on the blades. Stepped electric

motors are becoming a popular means to control blade pitch. When elevated power levels are detected, the motors pitch the blades out of the wind, and when the power output is low, the blades are pitched into the wind [7]. This allows the turbine to feed the correct speed into the gearbox and generator in order to produce stable power.

1.3 Purpose

It is the purpose of this paper to investigate how pitch control alone affects a wind turbine's output power frequency at various wind speeds. I will answer the question: can pitch control alone regulate a wind turbine's rotational speed over a wide wind speed range? I will also investigate the difference between fixed speed and variable speed operation. To do this I designed a small wind turbine with variable pitch blades and tested it in UCSC's wind tunnel.

Section 2 describes the structure of the wind tunnel and wind turbine as well as the devices for measuring wind speed and rotational speed. The methods for measuring these values are explained in section 3. The data are analyzed in section 4 and conclusions from the data are explained in section 5.

2

Apparatus

2.1 The Wind Tunnel

An in-depth description of the wind tunnel's construction as well as photographs can be found in Part 2 of David Dawson's thesis [11]; it is summarized here for completeness.

The wind tunnel has a wooden exoskeleton for rigidity. The exoskeleton frames three sections: the compression section, test section, and exhaust section.

The compression section's frame is lined with smooth plastic sheeting and is boxed-in on the top and bottom by sheets of plywood. The plastic sheeting is stapled to the exoskeleton and all corners and edges are smoothed with Silicon II caulking.

The compression section feeds into the test section, a rectangular area with an inner cross-section measuring 12 ¼" wide by 9 ¼" tall. The sides are clear polycarbonate sheets and the top is a removable polycarbonate lid. The lid screws into aluminum brackets attached to the two side pieces and fits securely over foam seals lining the test section's opening.

Pulling the air through the wind tunnel are two 15-in. radiator fans. They are screwed into the exhaust section. Due to limited space, the fans point upward instead of in-line with the compression and test sections. Each fan is powered by a Raytheon DCR 40-25B 25A regulated power supply.

2.2 Measuring Flow Speed

A common way to measure changes in a fluid's velocity is to measure the change in the fluid's pressure and use Bernoulli's equation to relate the two [12]:

$$P_1 + \frac{1}{2}\rho v_1^2 + \rho g y_1 = P_2 + \frac{1}{2}\rho v_2^2 + \rho g y_2 .$$

For air flowing horizontally in the wind tunnel the height change is negligible, so Bernoulli's equation becomes

$$P_D + \frac{1}{2}\rho_{air} v_D^2 = P_S + \frac{1}{2}\rho_{air} v_S^2$$

where P_D, P_S, v_D, and v_S are dynamic pressure, static pressure, dynamic fluid velocity, and static fluid velocity respectively and ρ_{air} is the density of air.

Grouping similar terms and noting that $v_S = 0$ yields

$$v_D = \sqrt{\frac{2}{\rho_{air}}(P_S - P_D)} .$$

Thus air velocity in the wind tunnel can be determined from a device that measures a pressure differential.

One such device is called a pitot-static tube. A pitot-static tube (as seen in Fig. 2.1) consists of two tubes pointing into the fluid flow. One tube has an opening in the front to allow the fluid to flow directly into the tube, measuring the dynamic pressure. The other has an opening perpendicular to the flow; this tube measures the fluid's static pressure. The tubes lead to a flow meter which measures the pressure differential and displays fluid velocity.

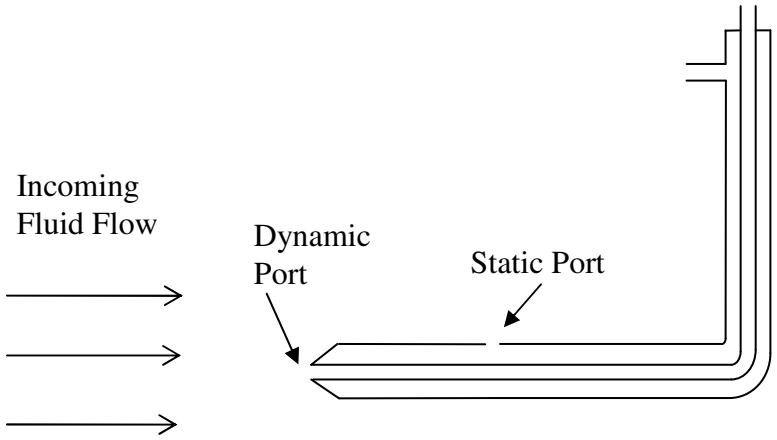

Figure 2.1: Pitot-Static Tube. The fluid flows left-to-right, across the static port and into the dynamic port.

The meter used is a Dwyer #460 Air Meter (see Fig. 2.2 below). The static and dynamic pressure inputs pull a small white ball up a central tube. The meter has a low-speed scale on the left of the tube and a high-speed scale on the right (both scales are in feet per minute). To use the high speed scale, the left input connector must be plugged.

Figure 2.2: Dwyer #460 Air Meter [13].

2.3 The Wind Turbine

The wind turbine (see Fig. 2.3 below for a rendered image) is a horizontal-axis turbine with three blades. The 9 ¼”-tall test section limits the turbine’s rotor diameter to 7 ¾” leaving a ¾” margin of safety between the blade tips and the top and bottom of the test section. The test section’s small size limits blade selection to model aircraft propellers. I chose APC Electric 7x5E blades because of their length and stock blade pitch (the desired pitch is explained later).

Each blade is bolted into a Microheli CNC Tail Rotor (hereafter called a blade grip). Since the model aircraft propeller blades are attached in pairs like real

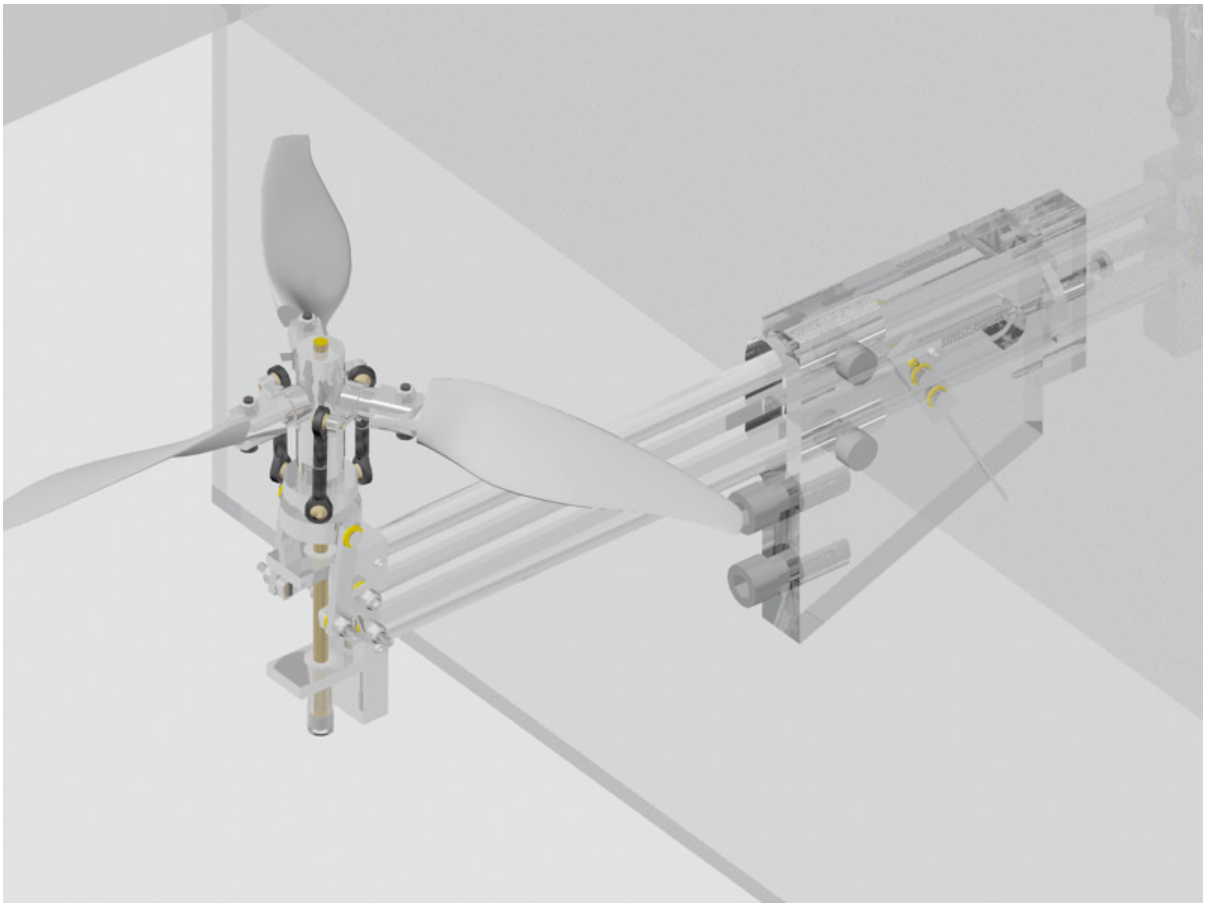

Figure 2.3: Rendering of wind turbine.

aircraft propellers, they must be cut in half and the inside ends shaved to fit into the blade grips.

The blade grips have a moment arm that extrudes in line with the slot for the propeller blade. Because of this, and because the design allows the blade grip to rotate forward by twenty degrees and backwards by fifty degrees, the propeller blades need to have a stock blade pitch between zero and twenty degrees. This allows the blades to always have a positive blade pitch throughout the blade grip's motion.

For a 7x5E propeller, the first number is the tip-to-tip distance (in inches), and the second number is the distance it moves forward in one revolution. The tangent of the propeller pitch is equal to the ratio of the second number and the circumference of the tip's path in one revolution. For this propeller, the pitch is 13 degrees, which is within the desired range.

The blade grips screw into a custom-designed main hub. The main hub is secured to the main shaft via three set screws and has three teeth evenly spaced that run parallel to the main shaft. These teeth mate with complimentary teeth on the pitch-control hub (pc hub). The pc hub fits over a bushing that allows linear motion along the main shaft with minimal friction.

A ball-link linkage system connects the pc hub to the arm on each blade grip; when the pc hub translates forward and backward, the blade grips rotate and thus change the pitch of the propeller blades.

A collar fits over a bearing that is pressed onto the bushing. The bearing isolates the collar from the bushing, shaft, and hubs' rotation. A linkage set connects the collar and an external thumb screw; when the thumb screw moves up and down, the collar is pushed forward and backward.

The linkage system has a pivot point that is bolted to the turbine's frame, and the main shaft is pressed into bearings which are also secured by the frame. Two aluminum rods connect the frame to an external piece of polycarbonate to keep the turbine from wobbling. Taped to this is a scale for the blade angle with increments of five degrees. A needle is attached to the linkage system and pivots at a point on the polycarbonate piece. Appendix B explains the mathematical relationship between the blade angle and the needle angle, Appendix C lists the Mathematica code used to calculate the needle gauge and all errors, and Appendix D has detailed engineering drawings of the turbine parts.

The wind turbine was designed with help from Dave Thayer and Darryl Smith from the UCSC machine shop and Bob Land and Rob Land from Aerotec Corp. All parts were machined at Aerotec Corp.

2.4 Rotational Speed

A 25-loop coil of 26 gauge copper wire is taped to the back frame extrusion such that the normal vector to the coil points to the 1/8-inch cube magnet's center. As the turbine and magnet spin, the magnetic flux through the coil oscillates, producing an induced emf. I used a Tektronix 2245A 100MHz oscilloscope and a scope probe to measure the emf.

This setup is conceptually similar to a simple ac generator. The magnetic flux is given by [12]

$$\Phi_B = BNA\cos(\omega t)$$

where B is the magnetic field strength, A is the area of the coil of wire, N is the number of turns in the coil, and ω is the magnet's angular speed. The induced emf is found by taking the negative derivative of the magnetic flux

$$\xi = -\frac{d\Phi_B}{dt} = BNA\omega\sin(\omega t).$$

Thus the more turns in the coil, the stronger the magnet, or the faster the turbine rotates the larger the signal. Since the angular speed will vary during testing, and the magnet is the strongest for its size and price, the coil must have the most turns possible to maximize the signal.

If N=25, B=1 Tesla (for a small neodymium magnet), and $A=\pi(3.5mm)^2$, then the expected peak voltage is 0.001ω V (ignoring the distance between the magnet and coil of wire) [14].

3

Procedure

The first step is to bolt the turbine's lid to the aluminum brackets on the sides of the test section. This assures that in case of an accident, the turbine parts cannot exit the test section and cause injury.

It is recommended that the turbine not rotate faster than 65Hz. This value is calculated as follows: the maximum rotational speed of an unmodified APC 7x4E propeller is 345Hz [15]. However since the propellers are all cut at the central point and machined thinner, the sheer stress from incident wind have a stronger effect on the blades. Sheer stress is inversely proportional to the cross-sectional area of the object that is perpendicular to the applied force. Cutting material from the blades has decreased the cross-sectional width to 18.7 percent of the original width (from 10.7mm to 2.00mm), thereby increasing the sheer stress during operation. Assuming a linear relationship between rotational speed and sheer stress and assuming that the maximum rotational speed listed above is equivalent to the maximum sheer stress for which the blade is rated, the maximum rotational speed for the modified propeller is equal to $0.187 \cdot 345\text{Hz}$, or 65Hz.

Safety is a concern, so it is important to vary the blade pitch and voltage (which regulates flow velocity) in a way that slowly increases the turbine's rotational frequency.

The desired procedure starts with the blade pitch set to 60 degrees and the power supplies at 4V. After the frequency for this configuration is recorded, the blade pitch is decreased in increments of five degrees until the pitch is equal to five degrees. For each setting the rotational frequency is measured with an oscilloscope and recorded. Then the blade pitch is returned to 60 degrees, and the power supplies' voltage is increased by 1V. The above process of decreasing the blade pitch by five degrees and then increasing the voltage to the wind tunnel is repeated and the data recorded.

Because the wind turbine generates turbulence in its wake and the pitot-static tube is mounted behind the turbine, reading the wind speed while the turbine is rotating will yield an inaccurate value. Thus to measure the wind speed associated with certain power supply voltages, the turbine is removed and the original lid is secured to the wind tunnel. Then the power supplies are set to the voltages for which data were previously taken, and the wind speed is measured on the air meter.

Due to turbulence from the wind tunnel, the method for measuring the air speed is to record the maximum and minimum readings over a 30-second period; these values define the errors and their average the data points for the measured air speed at each voltage.

4

Data and Analysis

4.1 Turbine Blade Angle Error

The machined turbine parts (see Appendix D for diagrams) have a tolerance of ±0.005in. (0.13mm). All part lengths and errors are listed in Appendix C. The errors translate to an uncertainty in the blade pitch for a given needle position.

To determine the uncertainty in blade pitch, start by choosing an angle for α (see Fig. B). Through calculations described in Appendix B this angle yields a value for the needle's angle with the horizontal, θ, and uncertainty in that angle. Then the values for θ plus and minus the upper and lower bounds respectively are input into a parametric CAD model of the linkage system in Fig. B. The differences in the new values for α in each case are recorded as the upper and lower error bounds. The values for α, θ, and their respective errors are listed in Table A.1 in Appendix A.

4.2 Flow Speed and Rotational Speed

With the original lid on the wind tunnel and no obstructions in the test section, the air speed for each power supply voltage setting is measured in feet per minute. The air speed, converted to m/s, for each voltage setting is listed in Table 4.1.

The turbine's rotational frequency for every voltage setting and blade pitch angle is listed in Tables A.2a,b. After measuring the frequency at several different

blade-pitch settings how to handle error on this measurement becomes a relevant question. For instance, at 3V and 55 degrees the turbine on average rotates at one revolution per second but at times stops rotating. Further measurements lead to the conclusion that the error is large when measuring the rotational frequency at a power supply voltage of 3V and that error increases as the turbine's speed increases.

Instead of attempting to measure the slowest and fastest frequency for every setting (the frequency fluctuates quickly compared to the oscilloscope's refresh rate), I approximated the error in discrete quantities that are proportional to the frequency. When measuring the frequency on the oscilloscope for frequencies less than 10Hz, the range of observed frequencies varies by at most 1Hz. The error for frequencies less than 10Hz is ±0.5Hz. By the same observation, the error

Power Supply Voltage (Volts)	Air Flow Speed (m/s)
3	1.83±0.10
4	2.39±0.15
5	3.00±0.25
6	3.76±0.30
7	4.72±0.36
8	5.49±0.30
9	6.6±0.5
10	7.1±0.5
11	7.9±0.8
12	8.9±0.8
13	9.7±1.0
14	11. ±1.3
15	12. ±1.0
16	13. ±1.3

Table 4.1: Measured air flow speed for each voltage setting. Air flow speeds for 3V-8V are measured on the low-speed scale, and air flow speeds for 9V-16V are measured on the high-speed scale.

for frequencies between 10Hz and 20Hz is ±1.0Hz, the error for frequencies between 20Hz and 30Hz is ±2.0Hz, and the error for frequencies between 30Hz and 40Hz is ±3.0Hz. Exceptions occur when the power supplies are set to 3V and when the measured frequency is less than 2Hz. In these situations the error is ±1.0Hz because the turbine's speed fluctuates more at this lower wind speed, and the small signal is difficult to measure on the oscilloscope.

4.2.1 The Turbine at 5 Degrees

As seen in Table A.2b, at a constant wind speed the turbine spins faster as the blade angle decreases until the blade angle is set to 5 degrees. A possible reason for this is that, as explained in the introduction, wind turbines rotate slower, or 'stall,' at small blade angles. Stalling is a method that is not of interest in this paper, so the 5-degree data will be omitted in further data analysis. However, it is important to note that these data are in agreement with stall control as a method for decreasing the speed of a turbine.

4.2.2 Pitch Control and Fixed-Speed

For pitch control to effectively regulate a turbine's output power, it must be able to keep the turbine at a fixed rotational speed under a range of wind speeds. Suppose we want to keep the turbine rotating at 10Hz. It is not obvious what wind speed and blade pitch combinations will result in this rotational frequency from the measured data that are listed in Tables A.2a,b. Thus it is necessary to calculate best-fit curves for the data, one for each blade pitch. From these curves, we can

calculate, for each blade angle, the required wind speed to rotate the turbine at 10Hz.

I used LAB Fit's least squares method to fit the data to the equation

$$y = Ax^{1/3} + B .$$

The fit parameters are listed in Table A.3. We can now use these fits to calculate, for each blade angle, the wind speed necessary to rotate the turbine at 10Hz. LAB Fit has a method for extracting data from a best fit curve. This method creates a data table for a specified region of the best-fit curve, more specifically the region around 10Hz. The table lists the corresponding air flow speed and the error associated with the frequency. Then to find the error on the air flow speed, add the frequency error to 10Hz and determine the corresponding air flow speed; the difference between this speed and the previous one is the air flow speed error. The frequency error and air flow speed and error for each blade angle are listed in Table A.4.

The data agree with the expected: that larger blade angles require a faster wind speed to maintain a constant rotational speed. However a disagreement occurs between the 25- and 20-degree results. Here the data contradict the expected because the wind speed remains constant instead of decreasing. This could be because the turbine did not rotate with a blade angle less than 20 degrees under the slowest tested wind conditions. This does not agree well with the other data at this wind speed; the expectation is that the turbine should continue to rotate faster as the blade angle decreases. The data at the slowest wind speed and at a blade angle

less than 20 degrees are considered outliers, and the parameters for the best fit curves without these points are listed in Table A.5. By the same method described above the frequency and air flow speeds, excluding the outliers described above, are listed in Table A.6. The rotational frequency data without the outliers and best fit curves are graphed in Fig. 4.1 below.

The resulting wind speed for a 20-degree-and-smaller blade angle is now progressively slower than that for a blade angle of 25 degrees. This agrees with the expected relationship between blade pitch and wind speed, thereby validating the fits as a means to determine the air flow speed required at each blade angle to produce a 10Hz turbine rotation.

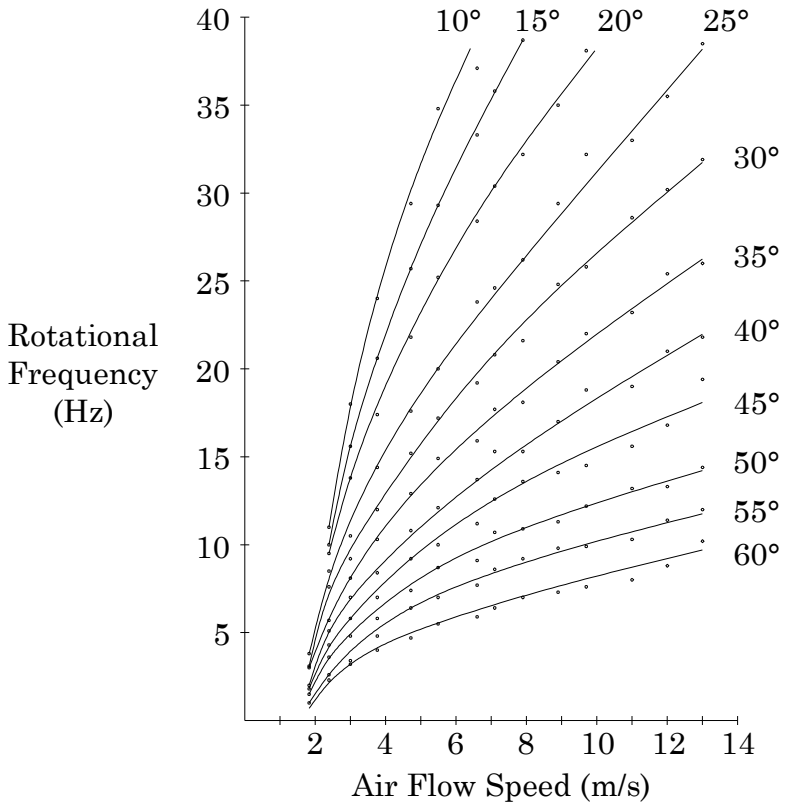

Figure 4.1: Rotational frequency vs. air flow speed data and best fit curve for every blade pitch angle.

The data in Table A.6 are graphed in Fig. 4.2 below. From this figure we can see how the blade angle is required to change under a range of wind speeds to maintain a constant rotational speed. Small wind changes at low wind speeds require larger adjustments to the blade angle, whereas small changes at higher wind speeds require relatively small adjustments to the blade angle. For example, when the wind speed increases from 2.2 m/s to 2.4 m/s the blade angle must increase by 10 degrees. However, if the wind speed was to increase from 9.3 m/s to 9.5 m/s (an equal change in wind speed as before), the blade angle will have to be increased by less than two degrees. A possible reason for this result is that since potential wind power is proportional to the cube of the wind speed, the potential wind power

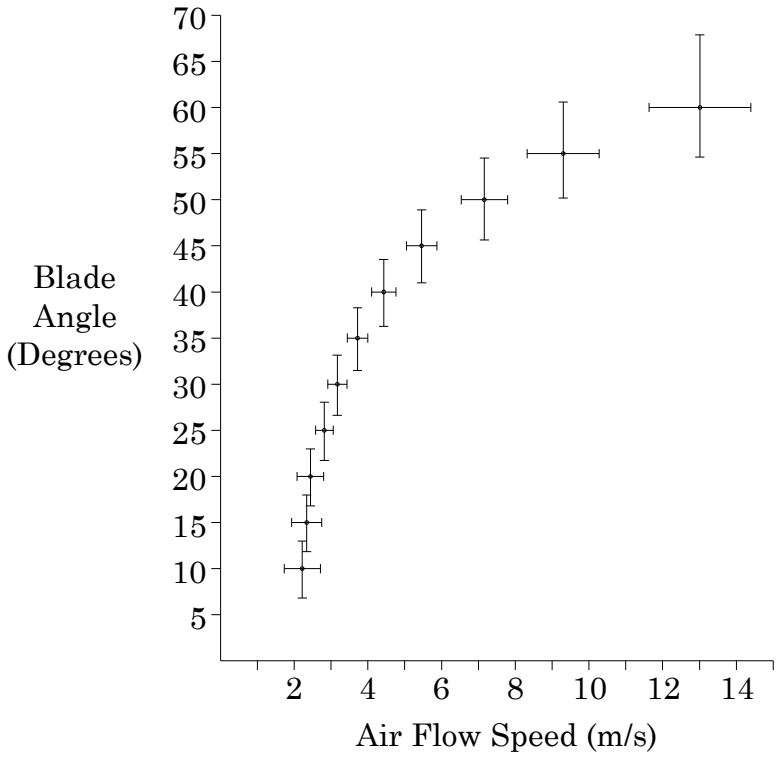

Figure 4.2: Blade angle vs. air flow speed to maintain a 10Hz turbine rotational frequency.

increases by 30 percent with the slower-wind-speed change but only increases by 6.6 percent with the faster-wind-speed change. Since the power harnessed by the wind turbine decreases as blade angle increases, it makes sense that the blade angle increase is greater for slower-wind-speed increases and vice versa.

4.3 Interpreting the Turbine's Rotation as Kinetic Energy

The kinetic energy of a rotating body is equal to

$$\mathrm{K} = \frac{1}{2} I \omega^2$$

where I is the moment of inertia (the rotational inertia), and ω is the angular frequency. Thus for a fixed-speed turbine rotating with angular frequency $2\omega f$ and moment of inertia I, we can calculate its kinetic energy and associate that energy as being proportional to the energy produced by the generator.

As the blade angle changes, the blades' moments of inertia change. Since the blades have complex shapes, they will be approximated as rectangular plates when calculating their moment of inertia. The blades are measured with digital calipers and the error in each measurement is assumed to be 0.2mm. The average width of a blade is determined by measuring the width at 15 evenly-spaced points along the blade. These widths are also used as a weight factor for determining the distance between the rotation axis and the center of mass, assuming the blades are of uniform thickness. The blades have a measured length of 72.7mm±0.2mm, an average width of 14.9mm±0.1mm and a center of mass displacement equal to

54.8mm±0.3mm. The mass of the blade is measured using a My-Weigh i500 scale to be 2.8g±0.1g.

The moment of inertia of the total blade approximation is given by

$$I = \frac{3}{12}\, \mathrm{m}\,(l^2 + \mathrm{w_{avg}}^2 \cos^2 \alpha_A) + 3\,\mathrm{m} l_{CM}^2$$

where m is the mass of the blade, l is the measured length, w_{avg} is the average width, α_A is the blade angle, and l_{CM} is the center of mass displacement. The calculated moment of inertia at each wind speed for the case where the turbine rotates at 10Hz is listed in Table 4.2.

The wind turbine's total moment of inertia is equal to three times the blade moment of inertia plus the moments of the other rotating parts. The moments from the other rotating parts do not vary as blade angle varies and so can be considered a constant. This constant will be omitted because the change in kinetic energy between wind speeds is more significant that the energy values themselves. If the

Wind Speed (m/s)	Moment of Inertia (kg·m²)	Kinetic Energy (Joules)
2.2±0.49	2.9E-5±1.1E-6	5.7E-2±5.4E-2
2.3±0.41	2.9E-5±1.1E-6	5.7E-2±3.8E-2
2.4±0.36	2.9E-5±1.1E-6	5.7E-2±2.4E-2
2.8±0.24	2.9E-5±1.1E-6	5.7E-2±1.4E-2
3.2±0.26	2.9E-5±1.1E-6	5.7E-2±1.1E-2
3.7±0.28	2.9E-5±1.1E-6	5.7E-2±9.5E-3
4.4±0.33	2.9E-5±1.1E-6	5.7E-2±8.1E-3
5.5±0.41	2.9E-5±1.1E-6	5.7E-2±7.3E-3
7.2±0.63	2.9E-5±1.1E-6	5.7E-2±7.5E-3
9.3±0.98	2.9E-5±1.1E-6	5.7E-2±8.1E-3
13.±1.4	2.9E-5±1.1E-6	5.7E-2±8.6E-3

Table 4.2: Calculated moment of inertia and kinetic energy for the turbine when rotating at 10Hz.

kinetic energy varies widely with wind speed, then a theoretical generator connected to this turbine will have an inconsistent output power. The kinetic energy associated with each wind speed is listed in Table 4.2.

The kinetic energy does not vary throughout the wind speed range. Thus with the proper automatic pitch control mechanism, the turbine has the potential to maintain a stable power input to drive a generator under varying wind conditions.

4.4 Variable Speed vs. Fixed Speed

The above calculation also allows for investigation of the difference between variable speed operation and fixed speed operation. Again we will assume that the ideal rotational frequency for this turbine is 10Hz. This means that a theoretical fixed speed version of this turbine will have a braking system (most likely electrical braking) to maintain its rotational frequency at 10Hz. The calculated energy difference between this theoretical turbine and the variable speed turbine is analogous to the amount of energy wasted by a braking mechanism.

For a chosen blade angle of 30 degrees, the variable speed kinetic energy and fixed speed kinetic energy are listed in Table 4.3. These values are calculated in the same way as in the previous section. For the fixed speed calculation the rotational frequency is equal to the measured value from the wind tunnel testing until that value exceeds 10Hz, after which the value is restricted to 10Hz. For the variable speed calculation the rotational frequency is always equal to that measured in the wind tunnel since it is left to freely rotate with the idea that the power output will be converted to grid quality power via power electronics.

The difference in energy is listed in the last column in Table 4.3. The calculated energy is larger for the variable speed case for most of the wind speed range. This means that restricting the speed of this turbine will waste energy at most wind speeds. This proves that variable speed turbines harness more wind power than fixed speed turbines at almost all wind speeds.

Wind Speed (m/s)	Variable Speed Kinetic Energy (Joules)	Fixed Speed Kinetic Energy (Joules)	Energy Difference (Joules)
1.83±0.10	5.5E-3±3.6E-3	5.5E-3±3.6E-3	0.0±5.1E-3
2.39±0.15	3.3E-2±4.5E-3	3.3E-2±4.5E-3	0.0±6.4E-3
3.00±0.25	4.9E-2±5.6E-3	4.9E-2±5.6E-3	0.0±7.9E-3
3.76±0.30	8.3E-2±1.4E-2	5.7E-2±2.1E-3	2.6E-2±1.4E-2
4.72±0.36	1.3E-1±1.8E-2	5.7E-2±2.1E-3	7.3E-2±1.8E-2
5.49±0.30	1.7E-1±2.1E-2	5.7E-2±2.1E-3	1.1E-1±2.1E-2
6.6±0.5	2.1E-1±2.3E-2	5.7E-2±2.1E-3	1.5E-1±2.3E-2
7.1±0.5	2.5E-1±4.9E-2	5.7E-2±2.1E-3	1.9E-1±4.9E-2
7.9±0.8	2.7E-1±5.1E-2	5.7E-2±2.1E-3	2.1E-1±5.1E-2
8.9±0.8	3.5E-1±5.8E-2	5.7E-2±2.1E-3	2.9E-1±5.8E-2
9.7±1.0	3.8E-1±6.1E-2	5.7E-2±2.1E-3	3.2E-1±6.1E-2
11. ±1.3	4.7E-1±6.8E-2	5.7E-2±2.1E-3	4.1E-1±6.8E-2
12. ±1.0	0.52±0.11	5.7E-2±2.1E-3	0.46±0.11
13. ±1.3	0.58±0.11	5.7E-2±2.1E-3	0.52±0.11

Table 4.3: Variable speed kinetic energy, fixed speed kinetic energy, and their difference for a turbine with a fixed blade angle equal to 30 degrees.

5

Conclusions

Pitch control has the ability to regulate a wind turbine's rotational speed. This translates to a steady power output from the generator. For small fluctuations in high-wind-speed conditions the required blade pitch change is also small; for small fluctuations in low-wind-speed conditions the necessary blade pitch change is much larger. This means that pitch control can have a strong impact on power quality in low-wind conditions. However this also means that the pitch control mechanism is more active in these conditions and uses more power. Therefore other methods to regulate a turbine's rotational speed might be more efficient than pitch control during low-wind conditions.

Variable speed operation is confirmed to harness more wind power than fixed speed operation. The variable speed power produced by a generator will decrease due to the frequency conversion process, but this is not a research interest in this paper.

One further research possibility is to investigate pitch control automation systems. This could involve detecting the turbine's rotational speed and then adjusting the blade angle via a servo connected to a programmable controller.

6

Bibliography

[1] Grogg, Kira. “Harvesting the Wind: The Physics of Wind Turbines.” 2005. <http://apps.carleton.edu/campus/library/digitalcommons/assets/pacp_7.pdf>.

[2] Rasila, Mika. “Torque- and Speed Control of a Pitch Regulated Wind Turbine.” 2003. <http://webfiles.portal.chalmers.se/et/MSc/RasilaMikaMSc.pdf>.

[3] EcoSys Energy Solutions. Google Image Search > horizontal wind turbine. April 2011<http://ecosysenergy.com/index.php?p=1_10_Wind>.

[4] Irish Energy News. Google Image Search > vertical wind turbine. April 2011 <http://irishenergynews.com/home/index.php/2010/10/08/husum-wind-energy-review/>.

[5] Global Energy Concepts. “Wind Turbine Technology Overview.” October 2005. <http://www.powernaturally.org/Programs/Wind/toolkit/9_windturbinetech.pdf>.

[6] David, Andrew S. “Wind Turbines Industry and Trade Summary.” United States International Trade Commission. June 2009. <http://www.usitc.gov/publications/332/ITS-2.pdf>.

[7] Ragheb, M. “Control of Wind Turbines.” Wind Power Systems Lecture 24. 6 May 2009. <https://netfiles.uiuc.edu/mragheb/www/

NPRE%20475%20Wind%20Power%20Systems/>.

[8] Stiesdal, Henrik. "The Wind Turbine Components and Operation Bonus Info." Autumn 1999. <http://www.windmission.dk/workshop/BonusTurbine.pdf>.

[9] Schmidt, Michael. "Wind Turbine Design Optimization." April 2010. <http://www.clemson.edu/scies/wind/Poster-Schmidt.pdf>.

[10] Fingersh, L. J., Robinson, M. C. "The Effects of Variable Speed and Drive Train Component Efficiencies on Wind Turbine Energy Capture." National Renewable Energy Laboratory. January 1997. <http://www.osti.gov/bridge/servlets/purl/656845-S4micG/webviewable/656845.pdf>.

[11] Dawson, David M. "Wind Tunnel Design and Testing With Applications to Aerodynamic Theory." May 2007.

[12] Giancoli, Douglas C. Physics for Scientists & Engineers. Upper Saddle River, NJ: Prentice Hall, 2000. 252, 311-312, 346, 740-741.

[13] Dwyer No. 460 Air Meter. Image. <http://www.flwleightonstone.com/dwyer/airmeter_no460.html>.

[14] Kuttner, Fred. Interview with Geno Viscuso. 4 March 2011.

[15] APC Suggested RPM Limits. <http://www.apcprop.com/v/html/rpm_limits.html>.

[16] Lyons, Louis. A Practical Guide to Data Analysis for Physical Science Students. New York, NY: University of Cambridge, 2003.

[17] Bertoline, Gary R. Introduction to Graphics Communications for Engineers. New York, NY: McGraw-Hill, 2009.

Appendix A: Wind Turbine Data

α	Blade Pitch, α_A	$\sigma_{\alpha A+}$	$\sigma_{\alpha A-}$	θ	$\sigma_{\theta+}$	$\sigma_{\theta-}$
13	0	3.09	3.31	39.7	2.17	2.32
8	5	3.04	3.23	35.9	2.43	2.59
3	10	3.00	3.18	31.7	2.71	2.88
-2	15	2.98	3.17	26.9	3.01	3.18
-7	20	3.00	3.19	21.6	3.32	3.48
-12	25	3.03	3.25	16.0	3.60	3.73
-17	30	3.10	3.34	10.0	3.83	3.92
-22	35	3.24	3.49	4.07	3.97	4.01
-27	40	3.46	3.69	-1.71	4.01	4.00
-32	45	3.81	3.94	-7.07	3.94	3.88
-37	50	4.37	4.28	-11.8	3.78	3.68
-42	55	5.33	4.71	-15.8	3.54	3.42
-47	60	7.24	5.27	-19.0	3.26	3.14

Table A.1: Needle angle and error for a given angle of attack. α is the angle between the blade grip's moment arm and vertical and is offset from the blade pitch by twelve degrees, the angle of the propeller blades. All values are measured in degrees.

Power Supply Voltage (Volts)	Measured Frequency (in Hz) at a blade angle of:					
	60º	55º	50º	45º	40º	35º
3	0	1.0±1.	1.5±1.	1.8±1.	2.0±1.	3.0±1.
4	2.3±0.5	2.6±0.5	3.6±0.5	4.3±0.5	5.1±0.5	5.7±0.5
5	3.2±0.5	3.4±0.5	4.8±0.5	5.8±0.5	7.0±0.5	8.1±0.5
6	4.0±0.5	4.8±0.5	5.8±0.5	7.0±0.5	8.4±0.5	10.3±1.0
7	4.7±0.5	6.4±0.5	7.4±0.5	9.2±0.5	10.8±1.0	12.9±1.0
8	5.5±0.5	7.0±0.5	8.7±0.5	10.0±1.0	12.1±1.0	14.9±1.0
9	5.9±0.5	7.7±0.5	9.1±0.5	11.2±1.0	13.7±1.0	15.9±1.0
10	6.4±0.5	8.6±0.5	10.7±1.0	12.6±1.0	15.3±1.0	17.7±1.0
11	7.0±0.5	9.2±0.5	10.9±1.0	13.6±1.0	15.3±1.0	18.1±1.0
12	7.3±0.5	9.8±0.5	11.3±1.0	14.1±1.0	17.0±1.0	20.4±2.0
13	7.6±0.5	9.9±0.5	12.2±1.0	14.5±1.0	18.8±1.0	22.0±2.0
14	8.0±0.5	10.3±1.0	13.2±1.0	15.6±1.0	19.0±1.0	23.2±2.0
15	8.8±0.5	11.4±1.0	13.3±1.0	16.8±1.0	21.0±2.0	25.4±2.0
16	10.2±1.0	12.0±1.0	14.4±1.0	19.4±1.0	21.8±2.0	26.0±2.0

Table A.2a: Turbine rotational speed for blade angles 60 degrees through 35 degrees.

Power Supply Voltage (Volts)	Measured Frequency (in Hz) at a blade angle of:					
	30°	25°	20°	15°	10°	5°
3	3.1±1.	3.8±1.	0	0	0	0
4	7.6±0.5	8.5±0.5	9.5±0.5	10.0±1.0	11.0±1.0	1.0±1.
5	9.2±0.5	10.5±1.0	13.8±1.0	15.6±1.0	18.0±1.0	17.3±1.0
6	12.0±1.0	14.4±1.0	17.4±1.0	20.6±2.0	24.0±2.0	21.2±2.0
7	15.2±1.0	17.6±1.0	21.8±2.0	25.7±2.0	29.4±2.0	26.0±2.0
8	17.2±1.0	20.0±2.0	25.2±2.0	29.3±2.0	34.8±2.0	32.4±3.0
9	19.2±1.0	23.8±2.0	28.4±2.0	33.3±3.0	37.1±3.0	-
10	20.8±2.0	24.6±2.0	30.4±3.0	35.8±3.0	-	-
11	21.6±2.0	26.2±2.0	32.2±2.0	38.7±3.0	-	-
12	24.8±2.0	29.4±2.0	35.0±3.0	-	-	-
13	25.8±2.0	32.2±3.0	38.1±3.0	-	-	-
14	28.6±2.0	33.0±3.0	-	-	-	-
15	30.2±3.0	35.5±3.0	-	-	-	-
16	31.9±3.0	38.5±3.0	-	-	-	-

Table A.2b: Turbine rotational speed for blade angles 30 degrees through 5 degrees.

α_A	A	B	σA	σB
60°	8.60	-10.2	0.38	0.59
55°	9.58	-10.2	0.66	1.2
50°	10.9	-11.0	0.74	0.13
45°	13.9	-14.4	0.82	1.4
40°	16.8	-17.6	0.98	1.6
35°	20.2	-21.2	1.1	1.9
30°	24.1	-25.4	1.4	2.2
25°	29.3	-31.3	1.6	2.5
20°	42.1	-49.5	2.5	3.7
15°	56.2	-68.5	1.7	2.2
10°	68.7	-83.8	2.3	2.9

Table A.3: Fit parameters and error for turbine rotational speed best fit curves.

α_A	Frequency (Hz)	Wind Speed (m/s)
60°	10.±0.73	13.±1.4
55°	10.±0.68	9.3±0.98
50°	10.±0.63	7.2±0.63
45°	10.±0.61	5.5±0.41
40°	10.±0.68	4.4±0.33
35°	10.±0.81	3.7±0.28
30°	10.±0.96	3.2±0.26
25°	10.±1.2	2.8±0.24
20°	10.±1.5	2.8±0.22
15°	10.±0.77	2.7±0.08
10°	10.±0.90	2.6±0.07

Table A.4: Wind speed and error for a constant, 10-Hz turbine rotational frequency.

α_A	A	B	σA	σB
60°	8.60	-10.2	0.38	0.59
55°	9.58	-10.2	0.66	1.2
50°	10.9	-11.0	0.74	0.13
45°	13.9	-14.4	0.82	1.4
40°	16.8	-17.6	0.98	1.6
35°	20.2	-21.2	1.1	1.9
30°	24.1	-25.4	1.4	2.2
25°	29.3	-31.3	1.6	2.5
20°	35.3	-37.5	2.7	4.3
15°	43.8	-48.1	4.1	6.4
10°	51.6	-57.3	6.0	9.1

Table A.5: Fit parameters and error for turbine rotational speed best fit curves excluding outliers.

α_A	Frequency (Hz)	Wind Speed (m/s)
60º	10.±0.73	13.±1.4
55º	10.±0.68	9.3±0.98
50º	10.±0.63	7.2±0.63
45º	10.±0.61	5.5±0.41
40º	10.±0.68	4.4±0.33
35º	10.±0.81	3.7±0.28
30º	10.±0.96	3.2±0.26
25º	10.±1.2	2.8±0.24
20º	10.±2.1	2.4±0.36
15º	10.±3.3	2.3±0.41
10º	10.±4.7	2.2±0.49

Table A.6: Wind speed and error for a constant, 10-Hz turbine rotational frequency, excluding outliers.

Appendix B: Converting Blade Pitch to Needle Angle

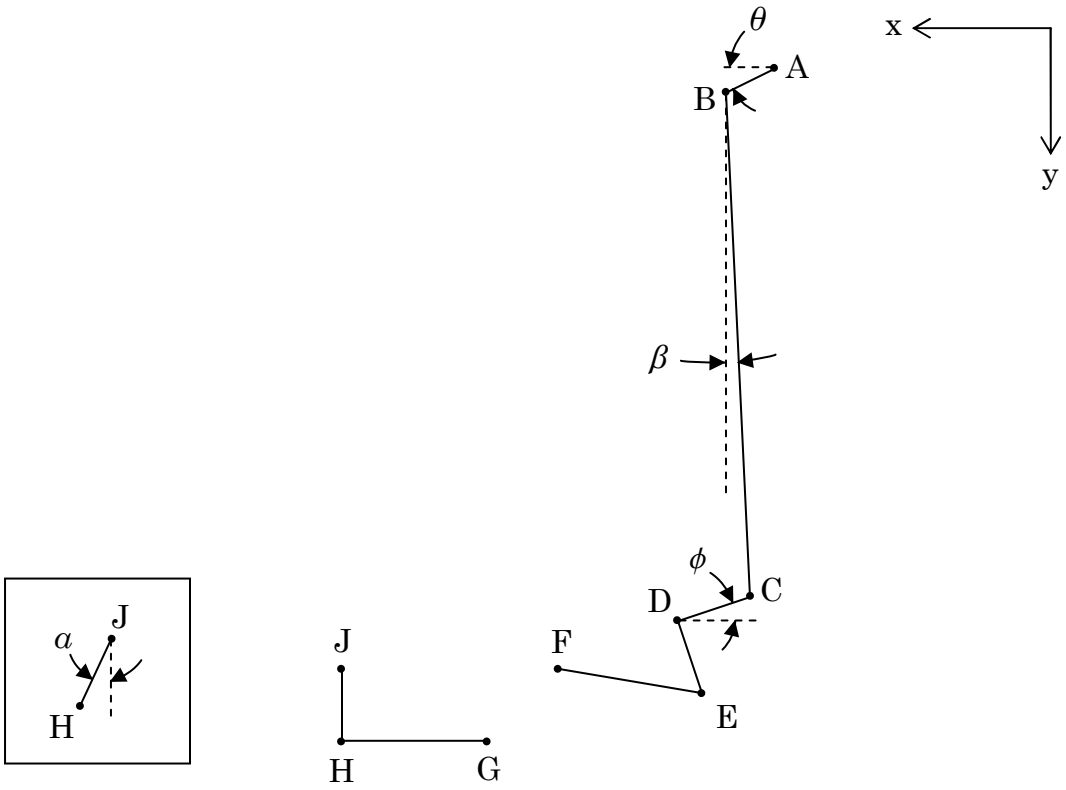

Figure B: Turbine blade pitch linkage system in 2-dimensions (not to scale). $\mathbf{r}_{AB}$ is the vector inline with the needle, point D is the pivot point on the frame, the blade grips bolt into the hub at point J, and $\mathbf{r}_{HJ}$ is the vector for the moment arm on the blade grips.

Measured Values (mm):	Points (mm):
$\lvert\mathbf{r}_{BC}\rvert$=146.35±0.13	$(A_x,A_y)=(0,0)$
$\lvert\mathbf{r}_{CD}\rvert$=8.99±0.13	$(B_x,B_y)=(7.29,B_y)$
$\lvert\mathbf{r}_{DE}\rvert=\lvert\mathbf{r}_{CD}\rvert$	$(D_x,D_y)=(13.56,151.79)$
$\lvert\mathbf{r}_{EF}\rvert$=20.59±0.13	$(F_x,F_y)=(F_x,157.6)$
$\lvert\mathbf{r}_{GH}\rvert$=22.3±0.4	$(G_x,G_y)=(F_x+7.3,F_y+\lvert\mathbf{r}_{HJ}\rvert)$
$\lvert\mathbf{r}_{HJ}\rvert$=8.95±0.2	$(J_x,J_y)=(62.1,157.6)$

Constraint #1: $(C_x, C_y) = (B_x - |\mathbf{r}_{BC}| \sin\beta, B_y + |\mathbf{r}_{BC}| \cos\beta)$

Since β is small, we can approximate sine and cosine by the first term in their Taylor expansion. Thus,

$$(C_x, C_y) \simeq (B_x - |\mathbf{r}_{BC}| \beta, B_y - |\mathbf{r}_{BC}|) \tag{B.1}$$

Also,

$(C_x, C_y) = -|\mathbf{r}_{CD}|(\cos\phi, \sin\phi) + (D_x, D_y)$ and $(E_x, E_y) = |\mathbf{r}_{DE}|(-\sin\phi, \cos\phi) + (D_x, D_y)$.

Moving the point (D_x, D_y) to the other side yields

$(C_x - D_x, C_y - D_y) = -|\mathbf{r}_{CD}|(\cos\phi, \sin\phi)$ and $(E_x - D_x, E_y - D_y) = |\mathbf{r}_{DE}|(-\sin\phi, \cos\phi)$.

Thus the relationship between point C and point E is

$$(E_x - D_x, E_y - D_y) = (C_y - D_y, D_x - C_x)$$

so

$$(E_x, E_y) = (C_y + D_x - D_y, -C_x + D_x + D_y). \tag{B.2}$$

Constraint #2: $(D_x - C_x)^2 + (D_y - C_y)^2 = |\mathbf{r}_{CD}|^2$

Solving for C_x yields

$$C_x = D_x - \sqrt{|\mathbf{r}_{CD}|^2 - (D_y - C_y)^2}\,. \tag{B.3}$$

Constraint #3: $(F_x - E_x)^2 + (F_y - E_y)^2 = |\mathbf{r}_{EF}|^2$

Substituting equation B.2 into this constraint yields

$$(F_x - C_y - D_x + D_y)^2 + (F_y + C_x - D_x - D_y)^2 = |\mathbf{r}_{EF}|^2.$$

Substituting equation B.3 into this yields

$$|\mathbf{r}_{EF}|^2 - (F_x - C_y - D_x + D_y)^2 = \left(F_y - D_y - \sqrt{|\mathbf{r}_{CD}|^2 - (D_y - C_y)^2}\right)^2.$$

Expanding the terms, rearranging, and then simplifying we obtain

$$2\,(D_y - F_y)\sqrt{|\,\mathbf{r}_{CD}\,|^2 - (D_y - C_y)^2} = |\,\mathbf{r}_{EF}\,|^2 - |\,\mathbf{r}_{CD}\,|^2 - (F_y - D_y)^2 - (F_x - D_x)^2 - 2\,(C_y - D_y)\,(D_x - F_x) \tag{B.4}$$

Equation B.4 is solved for C_y by using Mathematica's Solve command. After being simplified, the equation for C_y is found to be

$$\begin{aligned} Cy = & \Big((F_x - D_x)^3 + (F_x - D_x)\,(|\,\mathbf{r}_{CD}\,|^2 - |\,\mathbf{r}_{EF}\,|^2 + (D_y - F_y)^2) + \\ & 2\,D_y\,((D_x - F_x)^2 + (D_y - F_y)^2) - \\ & \Big(-(D_y - F_y)^2\Big(((D_x - F_x)^2 + (D_y - F_y)^2)^2 + (|\,\mathbf{r}_{CD}\,|^2 - |\,\mathbf{r}_{EF}\,|^2)^2 - \\ & \quad 2\,(|\,\mathbf{r}_{CD}\,|^2 + |\,\mathbf{r}_{EF}\,|^2)\,((F_x - D_x)^2 + (F_y - D_y)^2)\Big)\Big)^{1/2}\Big)\Big/ \\ & (2\,((D_x - F_x)^2 + (D_y - F_y)^2)) \end{aligned} \tag{B.5}$$

Method for determining F_x,

Constraint #4: $(H_x - J_x,\, H_y - J_y) = |\,\mathbf{r}_{HJ}\,|\,(\sin\alpha, \cos\alpha)$

Then,

$$(H_x,\, H_y) = (J_x + |\,\mathbf{r}_{HJ}\,|\sin\alpha,\, J_y + |\,\mathbf{r}_{HJ}\,|\cos\alpha) \tag{B.6}$$

Constraint #5: $(G_x - H_x)^2 + (G_y - H_y)^2 = |\,\mathbf{r}_{GH}\,|^2$

Substituting in (G_x, G_y) yields $(F_x + 7.3 - H_x)^2 + (F_y + |\,\mathbf{r}_{HJ}\,| - H_y)^2 = |\,\mathbf{r}_{GH}\,|^2$

Manipulating this results in the equation for F_x:

$$F_x = H_x - 7.3 - \sqrt{|\,\mathbf{r}_{GH}\,|^2 - (F_y + |\,\mathbf{r}_{HJ}\,| - H_y)^2} \tag{B.7}$$

Process for determining θ:

1. assign an angle to α
2. plug α into equation B.6

3. plug H_x and H_y into equation B.7

4. plug Fx into equation B.5

5. plug C_y into $B_y \simeq C_y - |\mathbf{r}_{BC}|$ (from equation B.1)

6. Finally, θ can be found via the equation

$$\theta = \tan^{-1}\left(\frac{B_y}{B_x}\right)$$

Appendix C: Mathematica Notebook

Clear[rBC, σrBC, rCD, σrCD, rDE, σrDE, rEF, σrEF, rGH, σrGH, rHJ, σrHJ, Bx, σBx, Dx, σDx, Dy, σDy, Fy, σFy, Gx, σGx, Gy, σGy, Jx, σJx, Jy, σJy, α, $\sigma\alpha$, Hx, Hy, σHx, σHy, Fx, σFx, Cy, σCy, By, σBy, θ, $\sigma\theta$upper, $\sigma\theta$lower]

$$Hx = Jx + rHJ * \text{Sin}[\alpha]$$

$$Hy = Jy + rHJ * \text{Cos}[\alpha]$$

$$\sigma Hx = (\sigma Jx^2 * (\partial_{Jx}\ Hx)^2 + \sigma rHJ^2 * (\partial_{rHJ}\ Hx)^2 + \sigma\alpha^2 * (\partial_{\alpha}\ Hx)^2)^{1/2}$$

$$\sigma Hy = (\sigma Jy^2 * (\partial_{Jy}\ Hy)^2 + \sigma rHJ^2 * (\partial_{rHJ}\ Hy)^2 + \sigma\alpha^2 * (\partial_{\alpha}\ Hy)^2)^{1/2}$$

$$Fx = Hx - 7.3 - \sqrt{rGH^2 - (Fy + rHJ - Hy)^2}$$

$$\sigma Fx = (\sigma Jx^2 * (\partial_{Jx}\ Fx)^2 + \sigma rHJ^2 * (\partial_{rHJ}\ Fx)^2 + \sigma\alpha^2 * (\partial_{\alpha}\ Fx)^2 + .2^2 + \sigma rGH^2 * (\partial_{rGH}\ Fx)^2 + \sigma Fy^2 * (\partial_{Fy}\ Fx)^2 + \sigma Jy^2 * (\partial_{Jy}\ Fx)^2)^{1/2}$$

$$Cy = \Big((Fx - Dx)^3 + (Fx - Dx) * (rCD^2 - rEF^2 + (Dy - Fy)^2) + 2 * Dy * ((Dx - Fx)^2 + (Dy - Fy)^2) - \big(-(Dy - Fy)^2 * \big(((Dx - Fx)^2 + (Dy - Fy)^2)^2 + (rCD^2 - rEF^2)^2 - 2 * (rCD^2 + rEF^2) * ((Fx - Dx)^2 + (Fy - Dy)^2)\big)\big)^{1/2}\Big) \Big/ (2 * ((Dx - Fx)^2 + (Dy - Fy)^2))$$

$$\sigma Cy = (\sigma Jx^2 * (\partial_{Jx}\ Cy)^2 + \sigma\alpha^2 * (\partial_{\alpha}\ Cy)^2 + .2^2 + \sigma rGH^2 * (\partial_{rGH}\ Cy)^2 + \sigma rHJ^2 * (\partial_{rHJ}\ Cy)^2 + \sigma Jy^2 * (\partial_{Jy}\ Cy)^2 + \sigma Dx^2 * (\partial_{Dx}\ Cy)^2 + \sigma Fy^2 * (\partial_{Fy}\ Cy)^2 + \sigma Dy^2 * (\partial_{Dy}\ Cy)^2 + \sigma rCD^2 * (\partial_{rCD}\ Cy)^2 + \sigma rEF^2 * (\partial_{rEF}\ Cy)^2)^{1/2}$$

$$By = Cy - rBC$$

$$\sigma By = \sqrt{\sigma Cy^2 + \sigma rBC^2}$$

$$\theta = \text{ArcTan}\Big[\frac{By}{Bx}\Big]$$

$$\sigma\theta\text{upper} = \sqrt{\Big(\theta - \text{ArcTan}\Big[\frac{By + \sigma By}{Bx}\Big]\Big)^2 + \Big(\theta - \text{ArcTan}\Big[\frac{By}{Bx + \sigma Bx}\Big]\Big)^2}$$

$$\sigma\theta\text{lower} = \sqrt{\Big(\theta - \text{ArcTan}\Big[\frac{By - \sigma By}{Bx}\Big]\Big)^2 + \Big(\theta - \text{ArcTan}\Big[\frac{By}{Bx - \sigma Bx}\Big]\Big)^2}$$

The above section stores equations for the location of each point described in appendix A and their respective error. Below each known length, point location, and error are defined.

$rBC = 146.35$
$\sigma rBC = .13$
$rCD = 8.99$
$\sigma rCD = .13$
$rDE = rCD$
$\sigma rDE = \sigma rCD$
$rEF = 20.59$
$\sigma rEF = .13$
$rGH = 22.3$
$\sigma rGH = .4$
$rHJ = 8.95$
$\sigma rHJ = .2$
$Bx = 7.29$
$\sigma Bx = 0$
$Dx = 13.56$
$\sigma Dx = 0$
$Dy = 151.79$
$\sigma Dy = 0$
$Fy = 157.6$
$\sigma Fy = 0$
$Gx = Fx + 7.3$
$\sigma Gx = \sqrt{\sigma Fx^2 + .2^2}$
$Gy = Fy + rHJ$
$\sigma Gy = \sqrt{\sigma Fy^2 + \sigma rHJ^2}$
$Jx = 62.1$
$\sigma Jx = 0$
$Jy = 157.6$
$\sigma Jy = 0$
$\alpha = 13 * 2 * \pi / 360$
$\sigma \alpha = 0$

After running this final section for a specified α Mathematica outputs several calculated points and their error as well as the needle angle and its upper and lower error.

Hx
Hy
σHx
σHy
Fx
σFx
Cy
σCy
By
σBy
$360 * \theta / (2 * \pi)$
$360 * \sigma\theta\text{upper} / (2 * \pi)$
$360 * \sigma\theta\text{lower} / (2 * \pi)$

Appendix D: Multiview and Assembly Drawings

Multiview drawings allow engineers, architects, and contractors to represent a three-dimensional object on a piece of paper. This is done by projecting the object onto orthogonal planes to create views such as front, top, bottom, right, and left. Visible lines are drawn with a thick line width, and hidden lines (lines that define edges hidden by the object in the current view) are thinner and have a dashed pattern. The views are dimensioned so that a machinist can recreate the object by looking at the plans. Care is taken to make sure to not over-dimension or under-dimension the object.

When a group of parts connect together they form an assembly. Assembly drawings detail how each part fits together. Assembly lines are used to show this. The parts are spread out on the paper, and the assembly is viewed from the top but at an angle, an isometric view.

The following pages include multiview drawings of each part that was either machined or modified and then assembly drawings of the turbine.

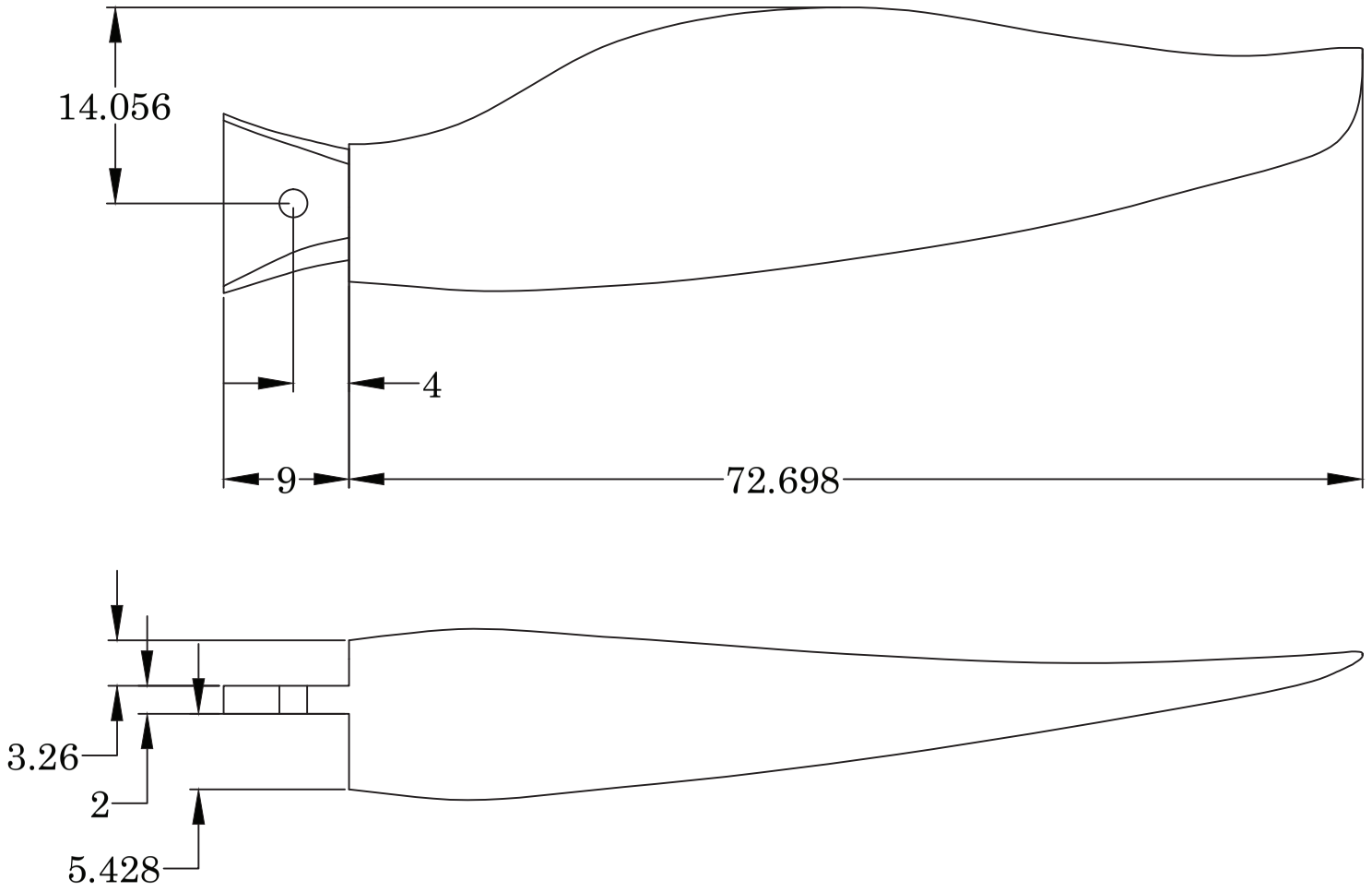

TURBINE BLADE SCALE 2:1

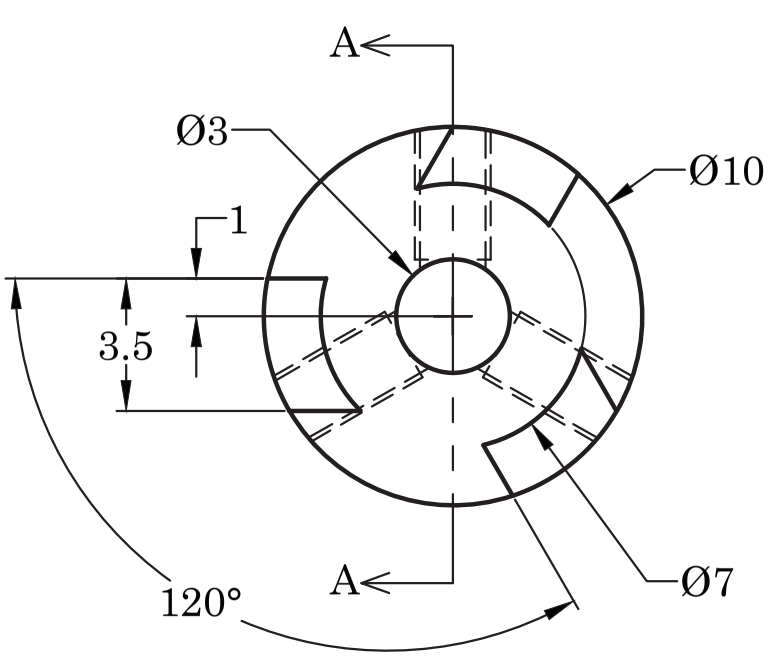

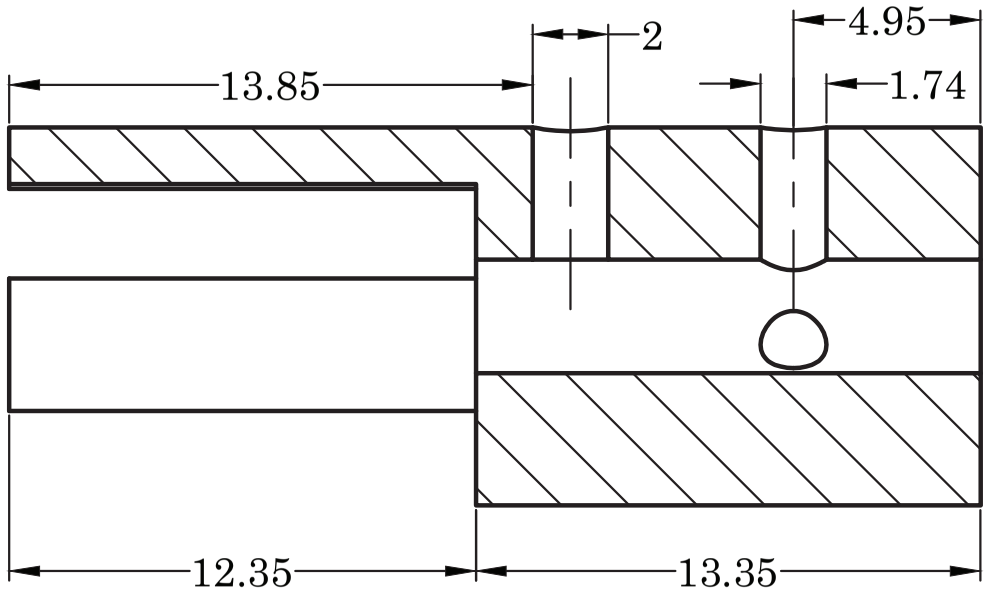

SECTION A-A

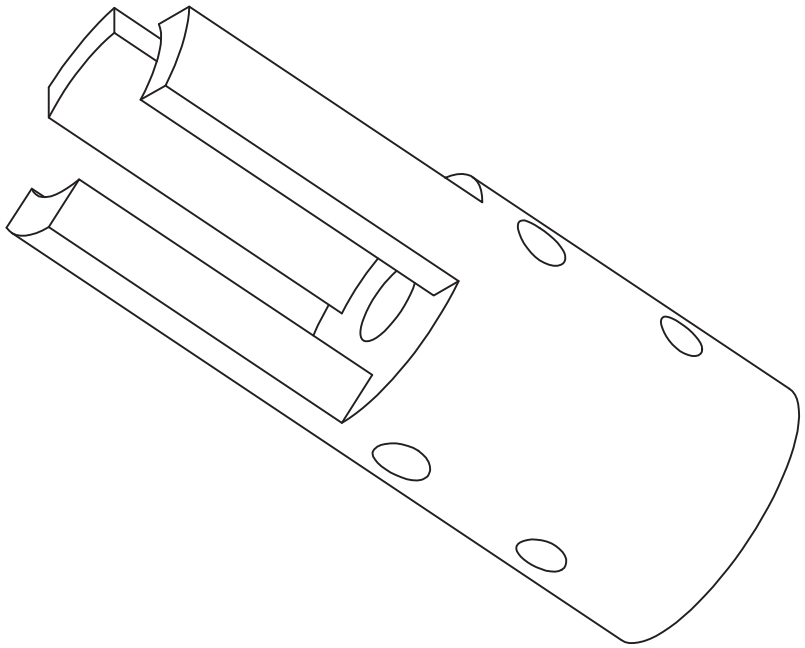

HUB SCALE 5:1

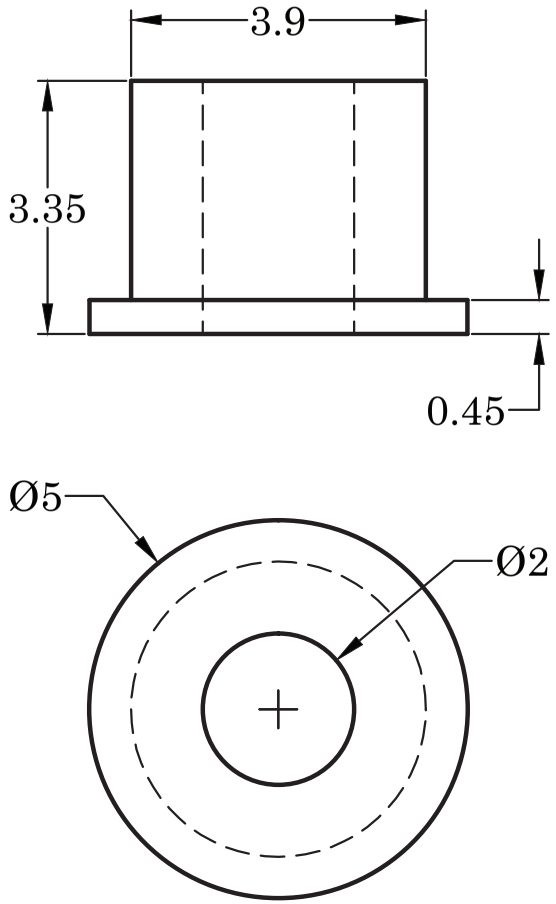

BLADE GRIP HAT INSERT SCALE 10:1

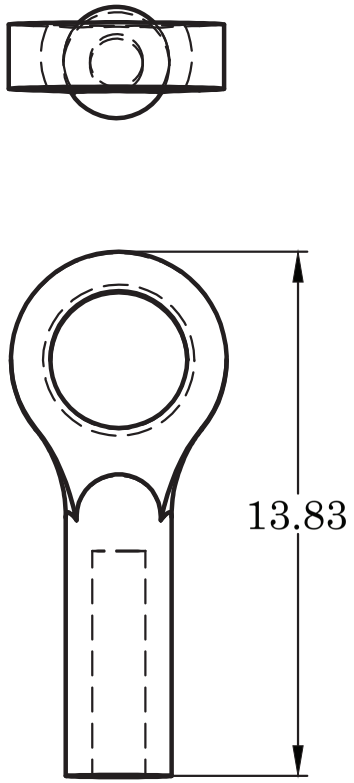

E-flite BALL LINK, CUT TO LENGTH SCALE 5:1

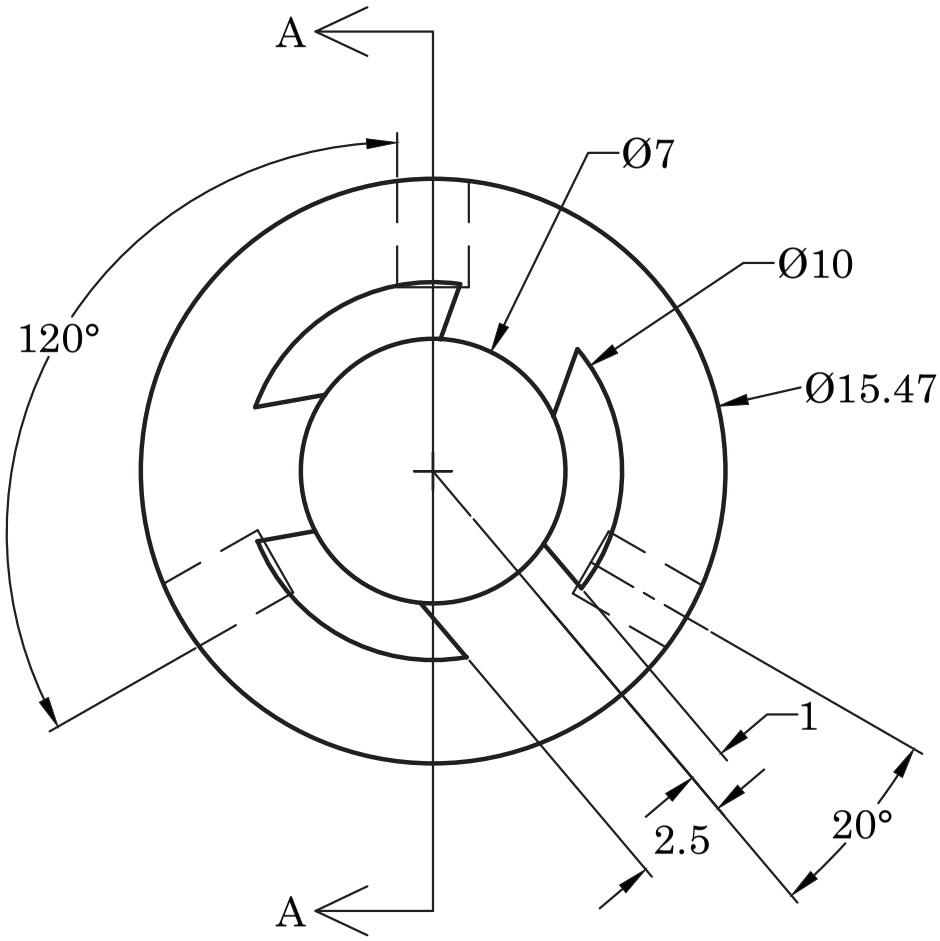

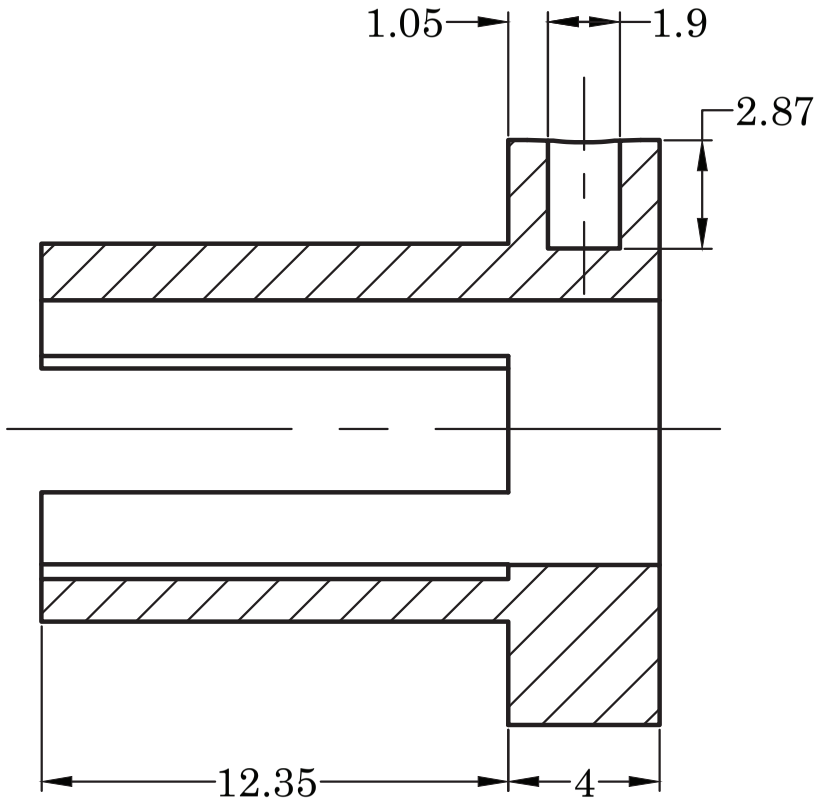

SECTION A-A

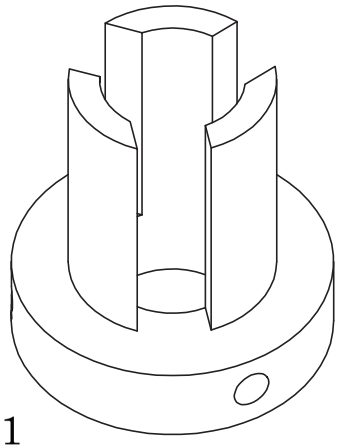

PITCH CONTROL HUB

SCALE 5:1

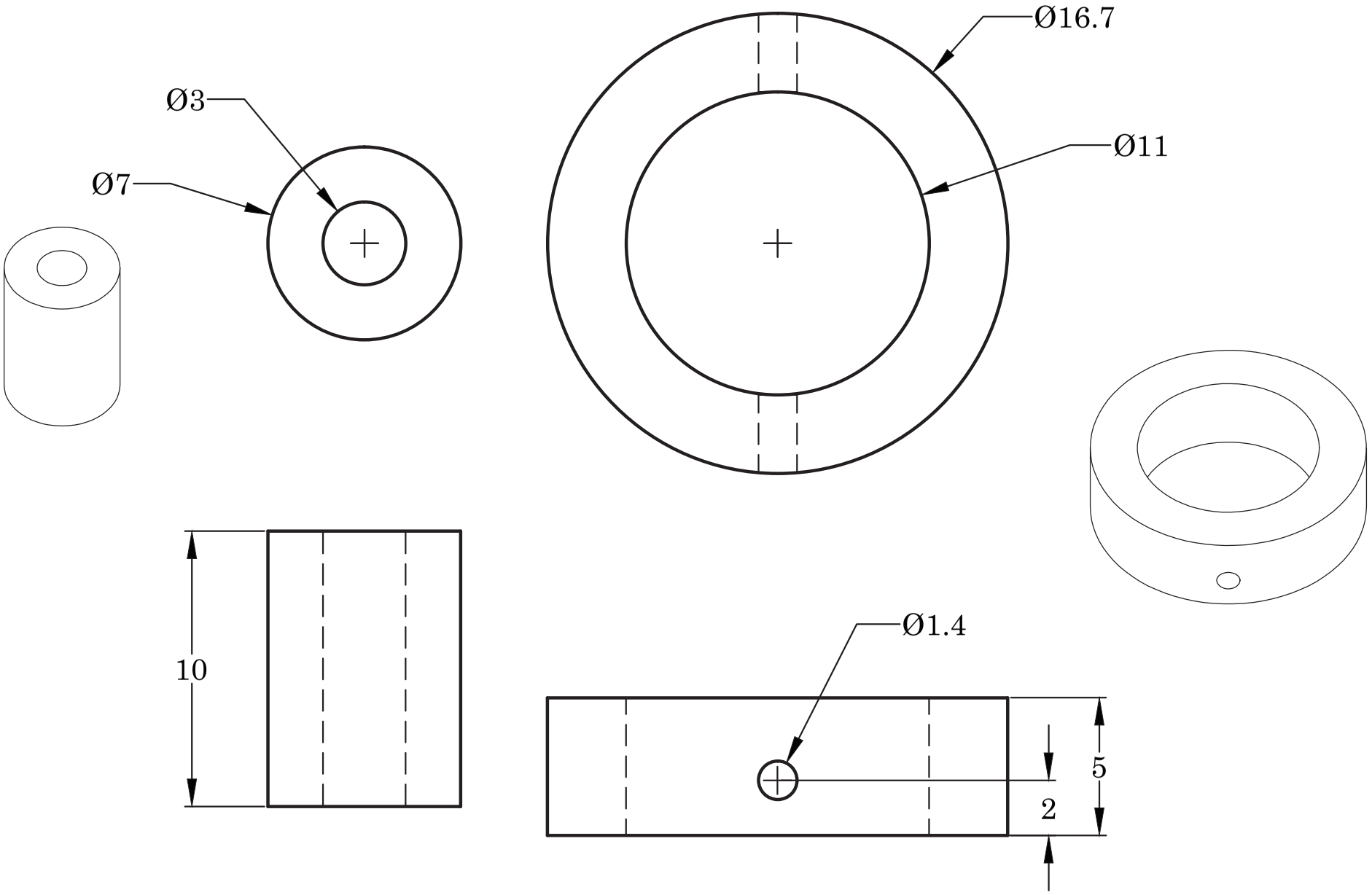

BUSHING SCALE 5:1 PITCH CONTROL BEARING COLLAR

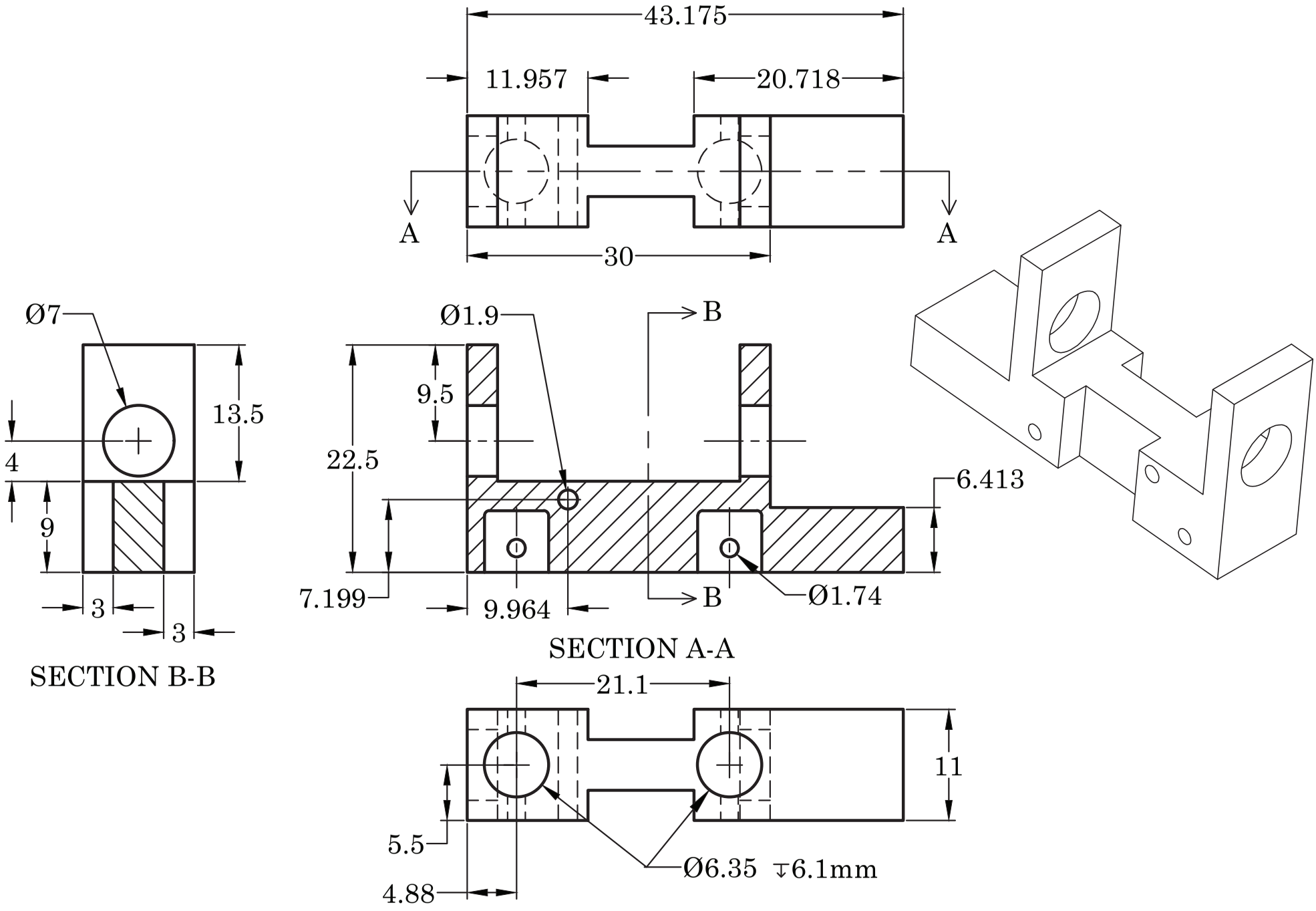

FRAME SCALE 2:1

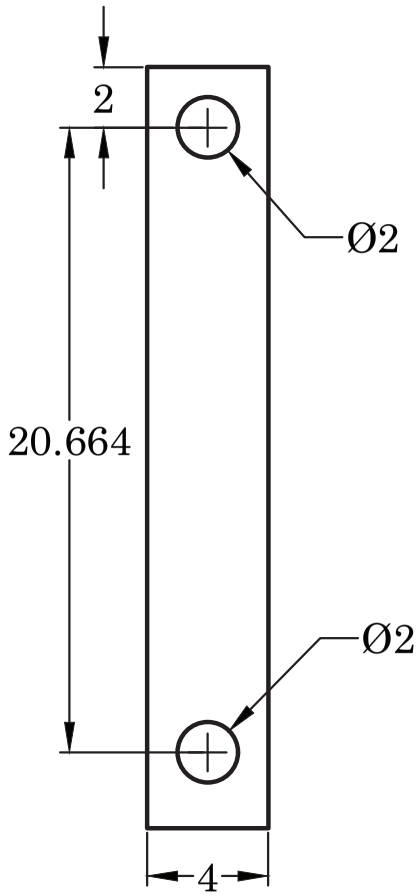

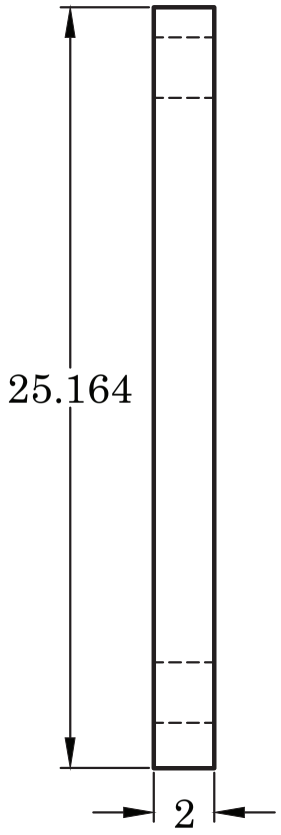

PUSH LINK SET SHORT ARM SCALE 4:1

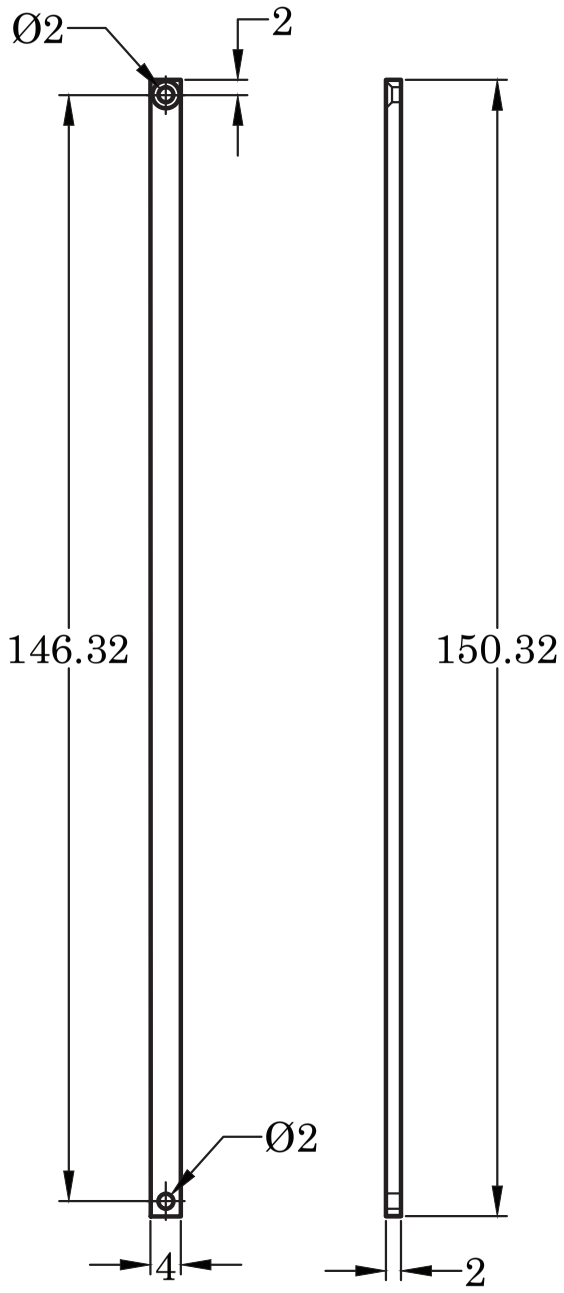

PUSH LINK SET LONG ARM SCALE 1:1

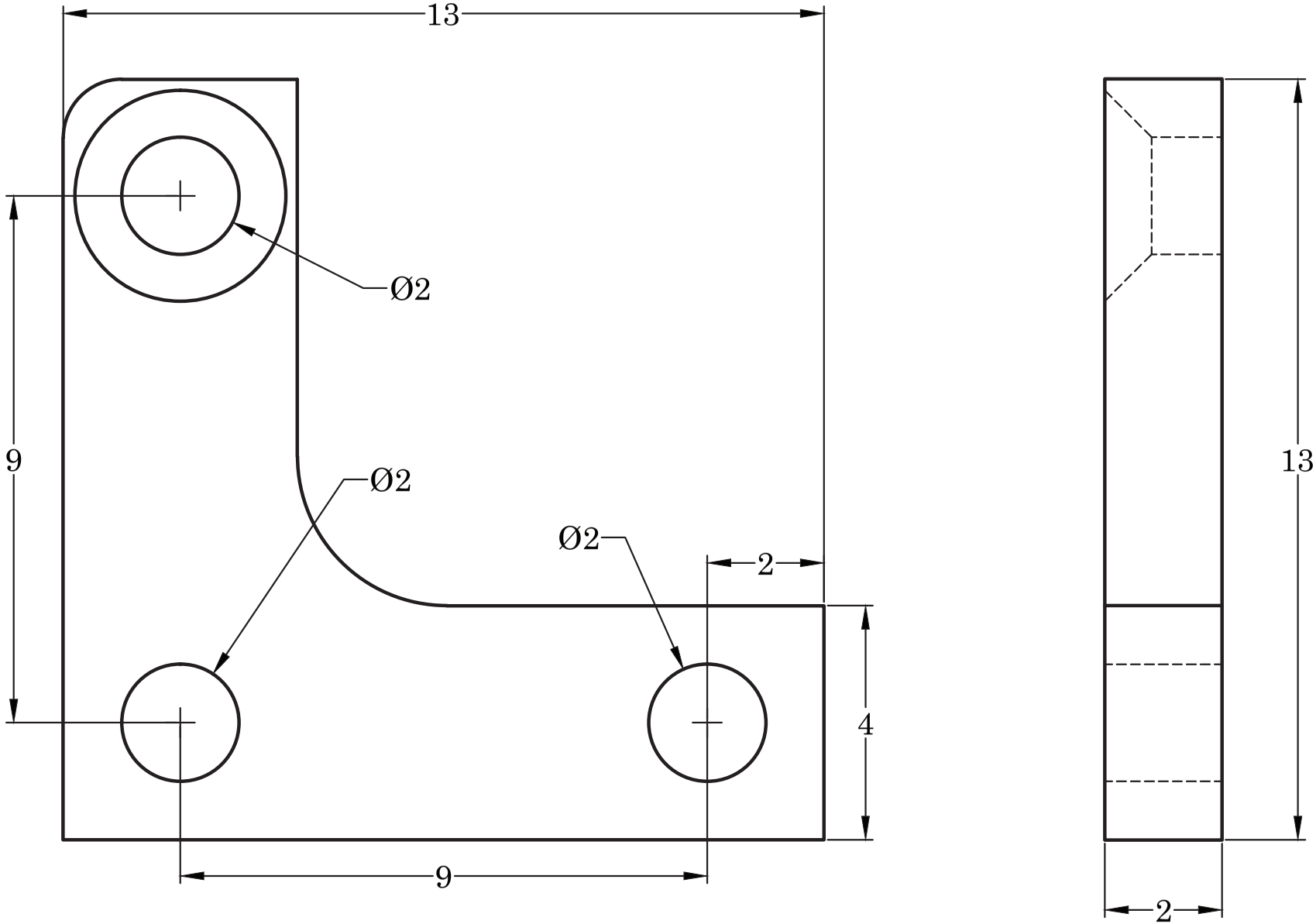

PUSH LINK SET 90°

SCALE 10:1

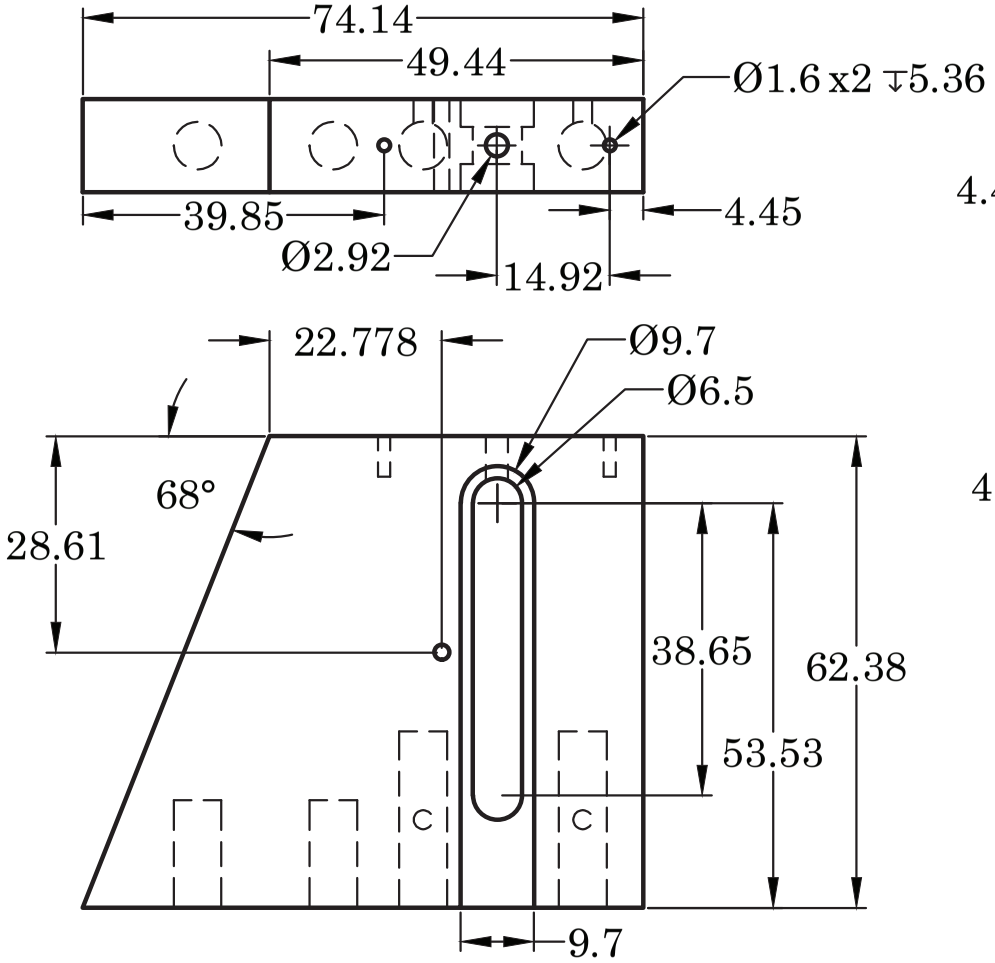

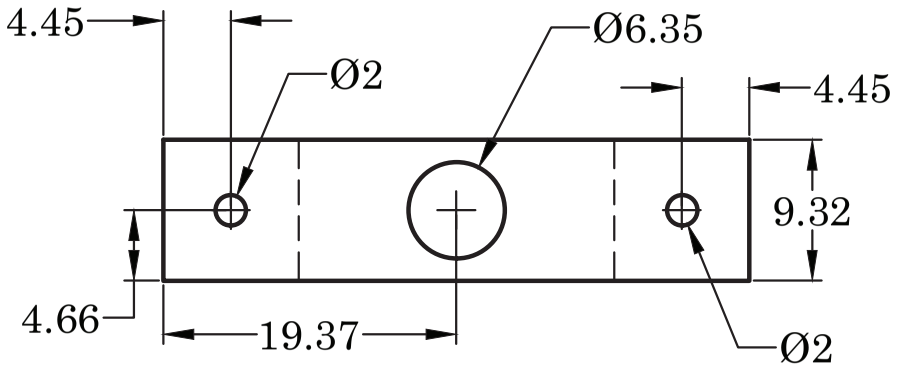

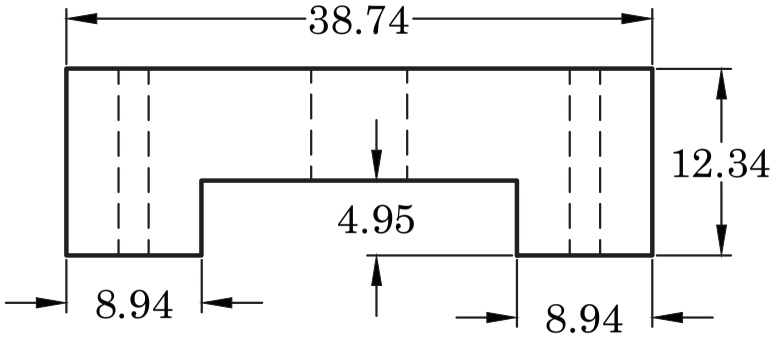

BEZEL KEEPER SCALE 2:1

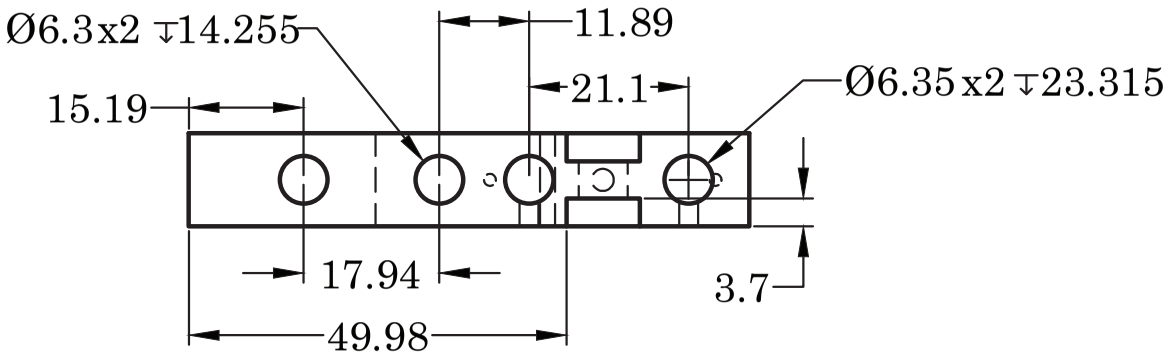

PITCH CONTROL BLOCK SCALE 1:1

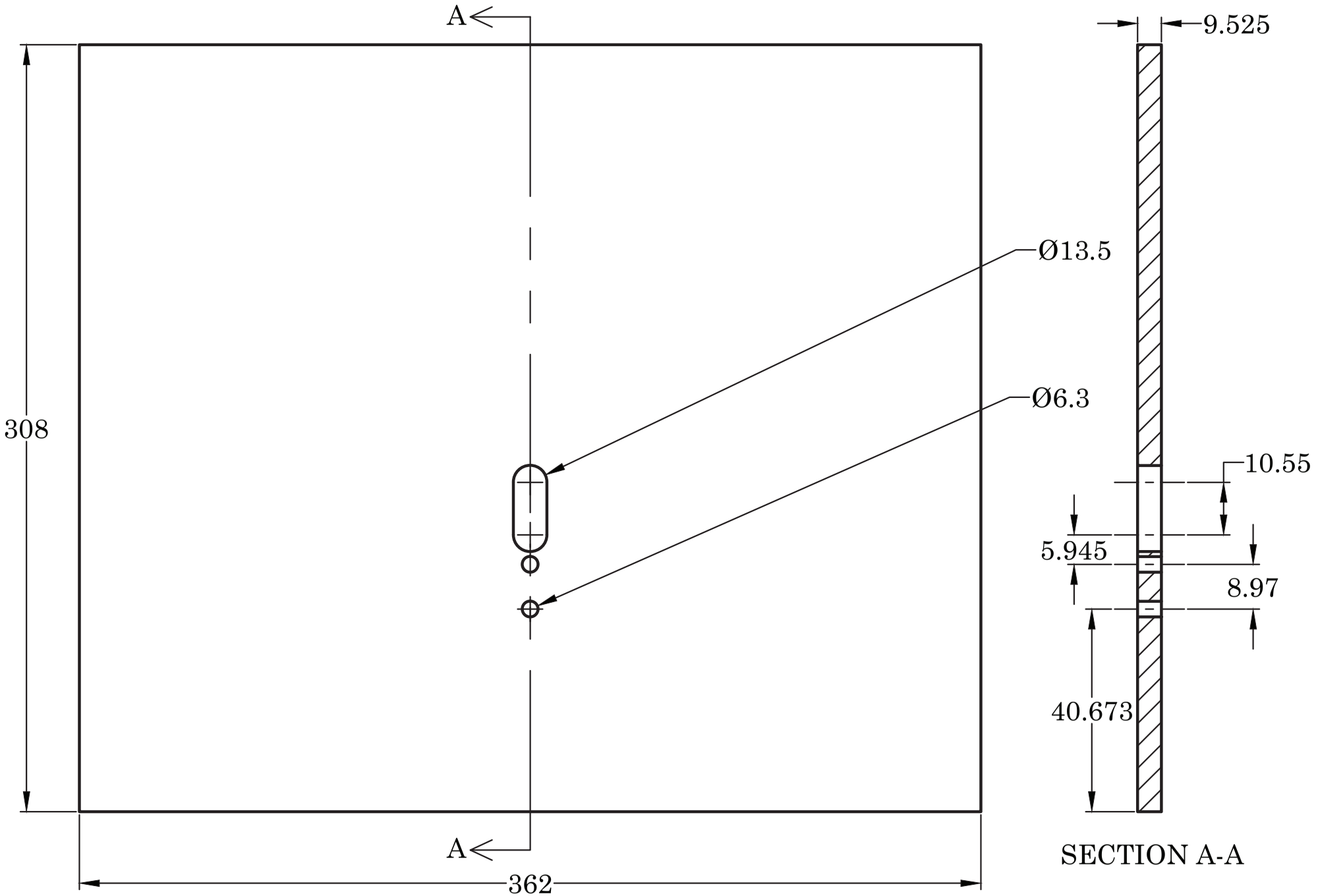
A
A
308
362
Ø13.5
Ø6.3
9.525
10.55
5.945
8.97
40.673
SECTION A-A

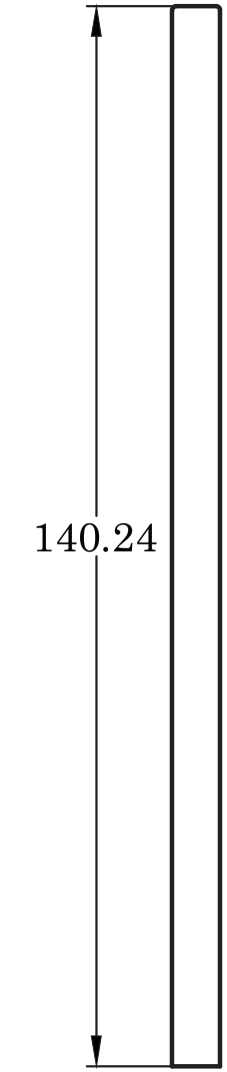

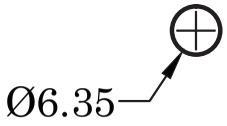

TOWER SCALE 1:1

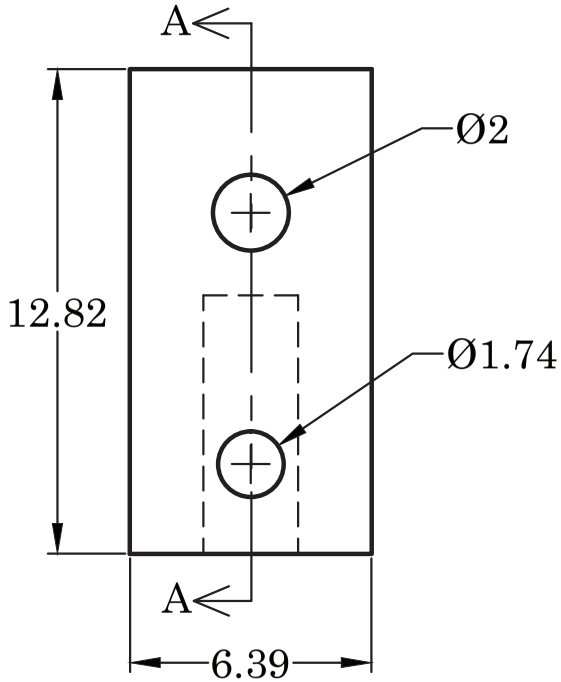

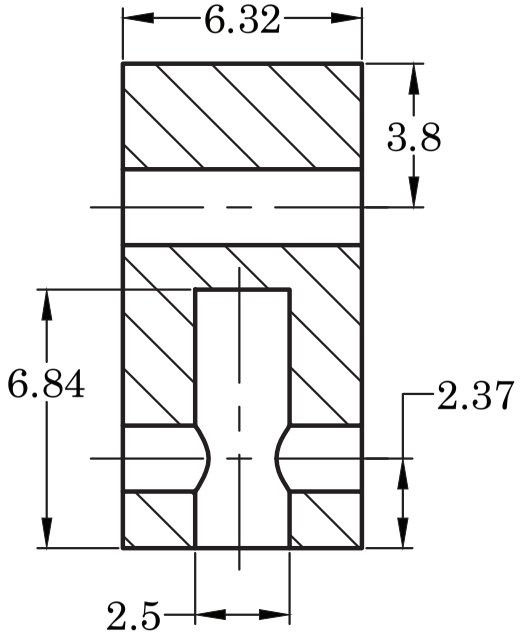

SECTION A-A

NEEDLE-PITCH CONTROL SET LINK SCALE 4:1

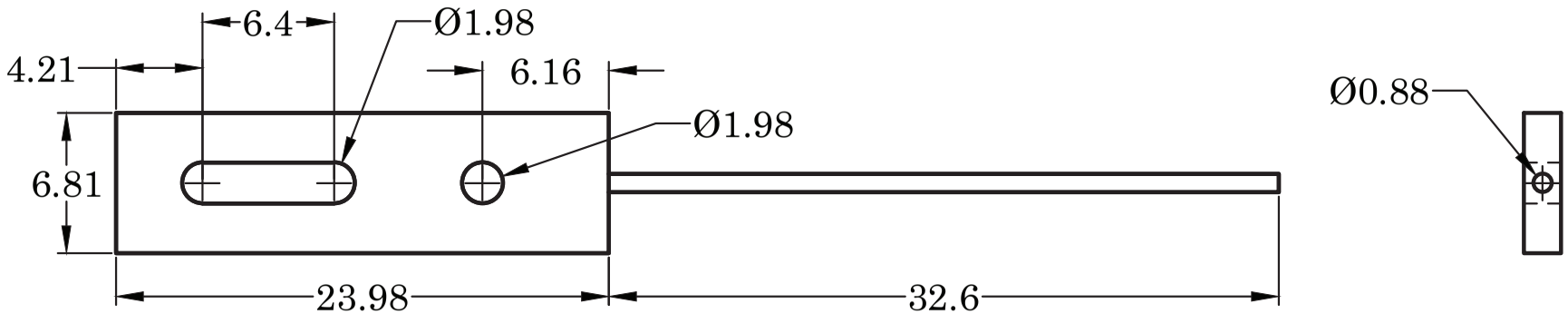

NEEDLE SCALE 3:1

ITEM	QTY	NAME	MATERIAL
1	1	PITCH CONTROL BLOCK	POLYCARBONATE
2	2	PUSH LINK SET LONG ARM	ALUMINUM
3	2	M2x0.4 NYLOC HEX NUT	STEEL
4	7	M2 WASHER 0.25mm	BRASS
5	1	2mm SPACER	STEEL
6	1	4-40 2" PAN HEAD SCREW	STEEL
7	4	M2x0.4 18mm PAN HEAD SCREW	STEEL
8	1	BEZEL KEEPER	POLYCARBONATE
9	1	BEZEL	ALUMINUM
10	1	COMPRESSION SPRING	STEEL
11	1	NEEDLE-PITCH CONTROL SET LINK	ALUMINUM
12	1	M2x0.4 3mm SET SCREW	STEEL
13	1	NEEDLE	ALUMINUM

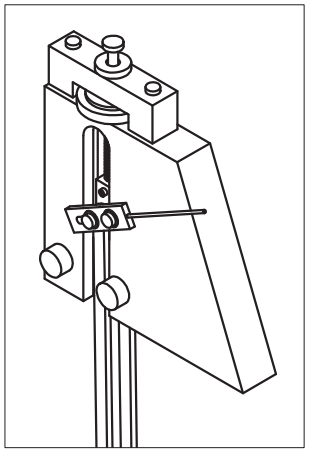

UPPER PITCH CONTROL SET ASSEMBLY

ITEM	QTY	NAME	MATERIAL
3	1	M2 0.4 NYLOC HEX NUT	STEEL
14	1	0-80x1.0" PAN HEAD SCREW, CUT TO 0.48"	STEEL
15	1	E-flite BALL LINK, CUT	PLASTIC
16	1	E-flite LINKAGE BALL SHORT	STEEL
17	1	BLADE GRIP HAT INSERT	ALUMINUM
18	1	Microheli TAIL ROTOR BLADE GRIP	ALUMINUM
19	1	APC 4Ex6 ELECTRIC PROPELLER, CUT	COMPOSITE
20	2	M2x0.4 10mm SOCKET HEAD CAP SCREW	STEEL

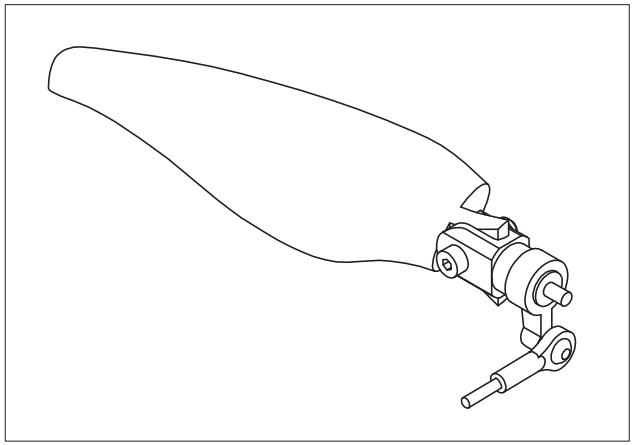

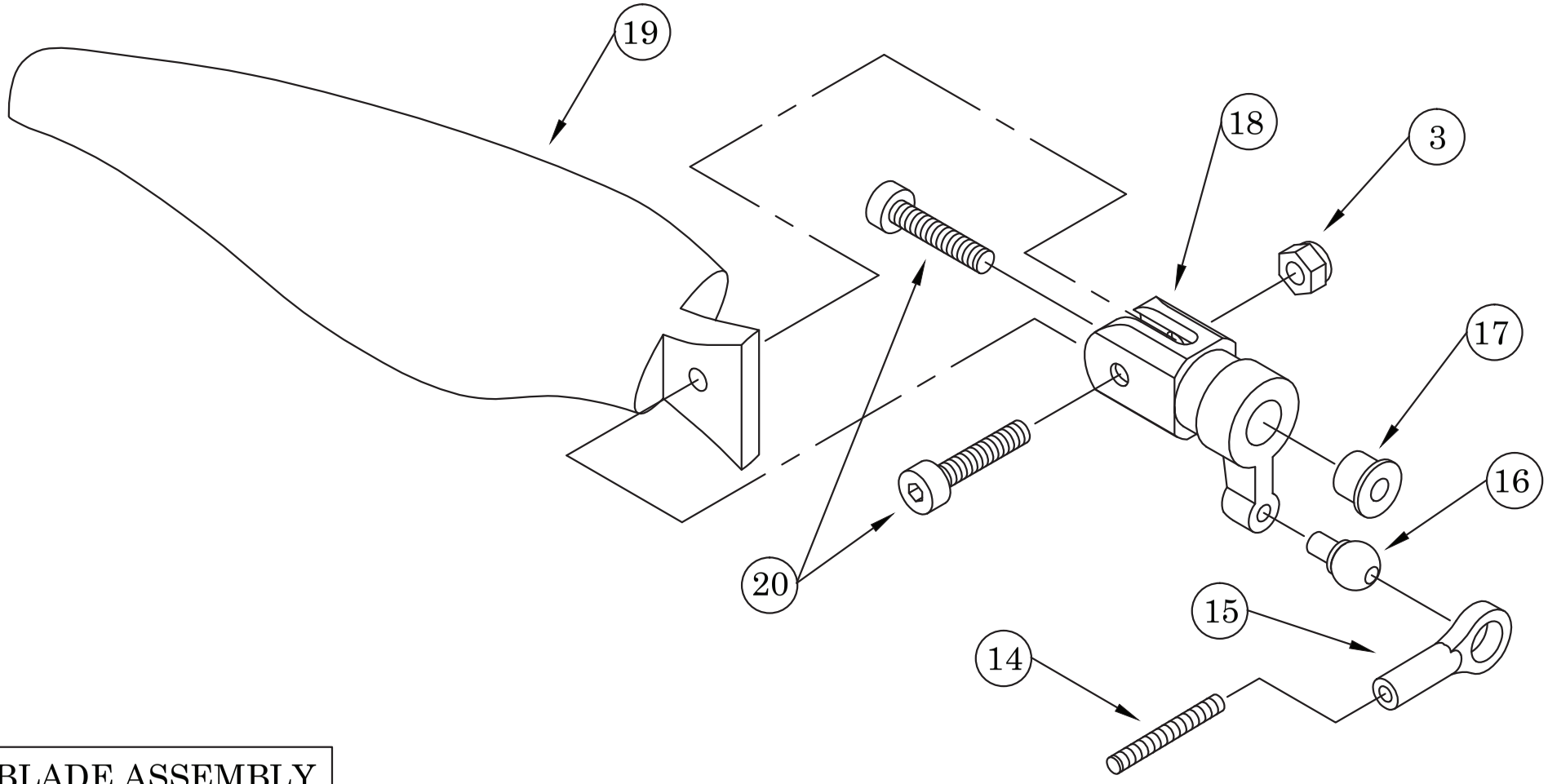

BLADE ASSEMBLY

ITEM	QTY	NAME	MATERIAL
4	2	M2 WASHER 0.25mm	BRASS
12	3	M2x0.4 3mm SET SCREW	STEEL
15	3	E-flite BALL LINK, CUT	PLASTIC
16	3	E-flite LINKAGE BALL SHORT	STEEL
21	1	HUB	ALUMINUM
22	1	PITCH CONTROL HUB	ALUMINUM
23	1	BUSHING	ALUMINUM
24	1	7x11x3 BALL BEARING	STEEL
25	2	M2x0.4 6mm FLAT HEAD SCREW	STEEL
26	2	PUSH LINK SET SHORT ARM	ALUMINUM
27	1	PC BEARING COLLAR	ALUMINUM
28	1	3mm O.D. 91.25mm MAIN SHAFT	BRASS

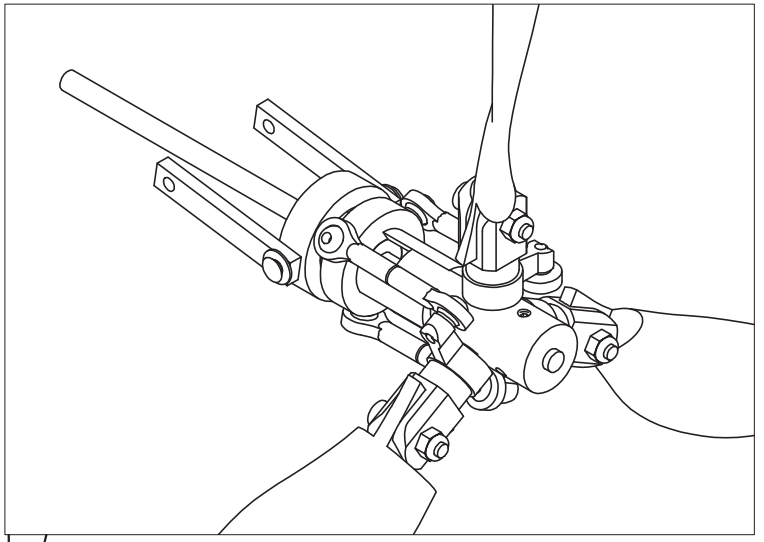

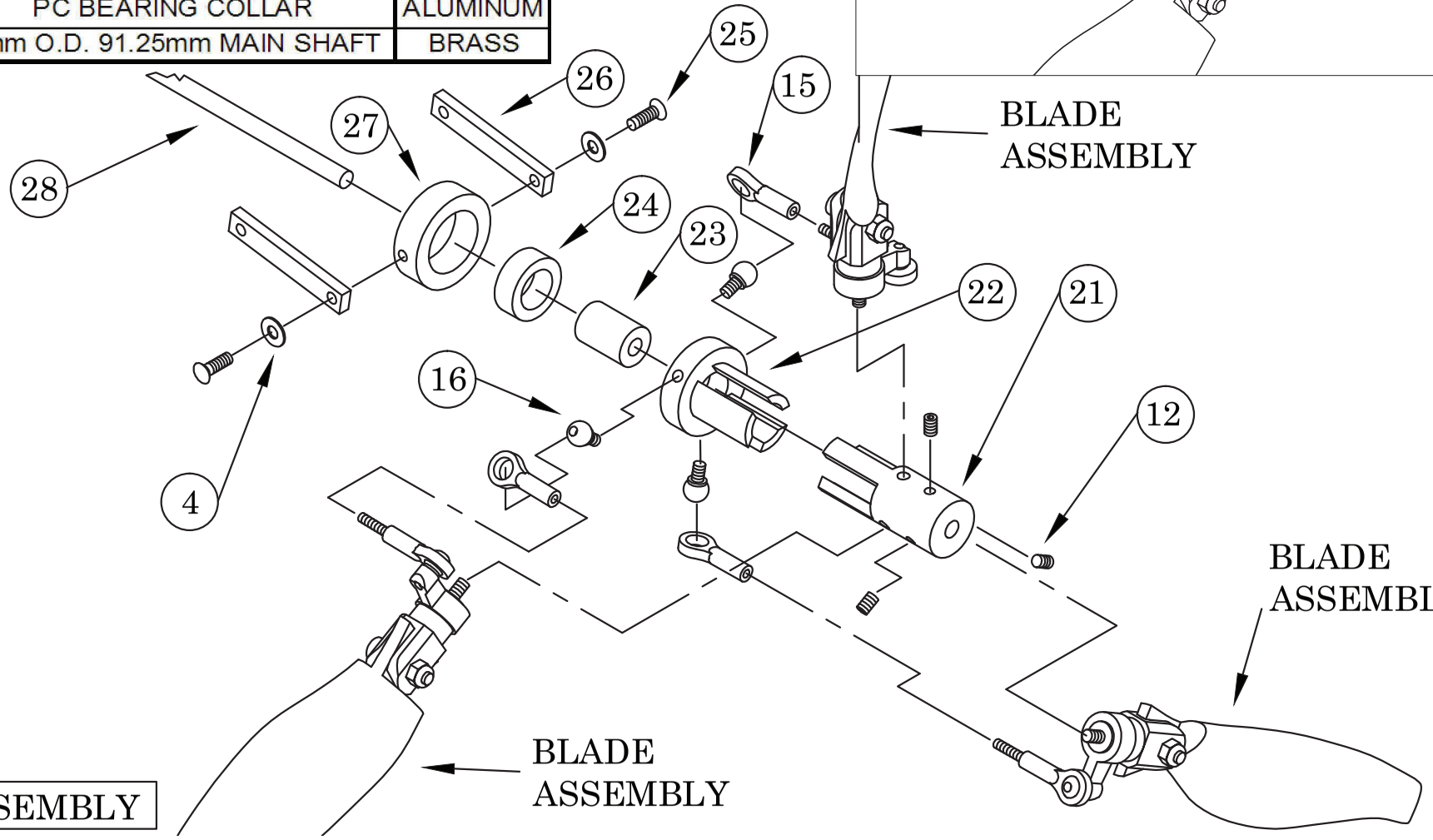

HUB ASSEMBLY

ITEM	QTY	NAME	MATERIAL
2	2	PUSH LINK SET LONG ARM	ALUMINUM
3	5	M2x0.4 NYLOC HEX NUT	STEEL
4	6	M2 WASHER 0.25mm	BRASS
7	1	M2x0.4 18mm PAN HEAD SCREW	STEEL
26	2	PUSH LINK SET SHORT ARM	ALUMINUM
29	2	PUSH LINK SET 90º	ALUMINUM
30	4	M2x0.4 10mm FLAT HEAD SCREW	STEEL
31	2	3x7x3 BALL BEARING	STEEL
32	1	FRAME	ALUMINUM

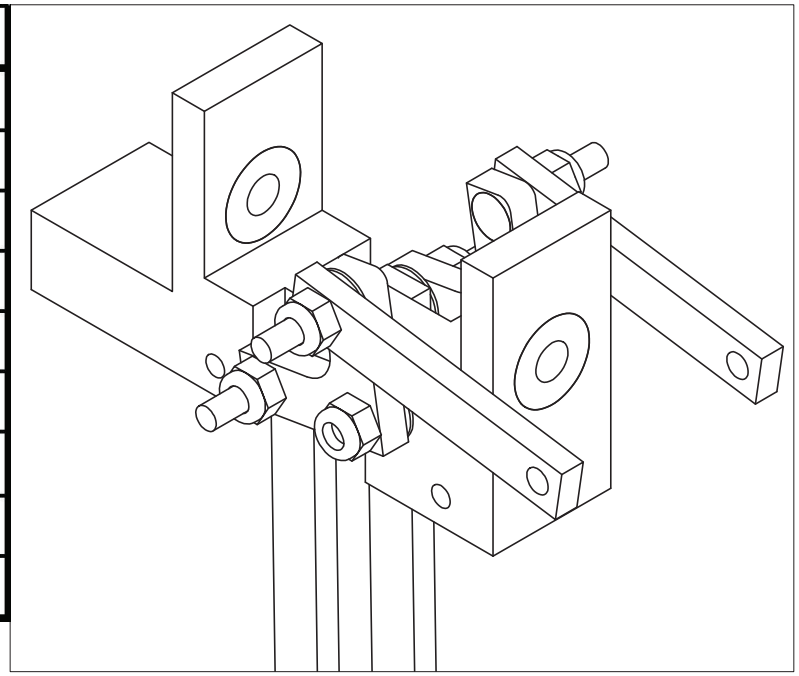

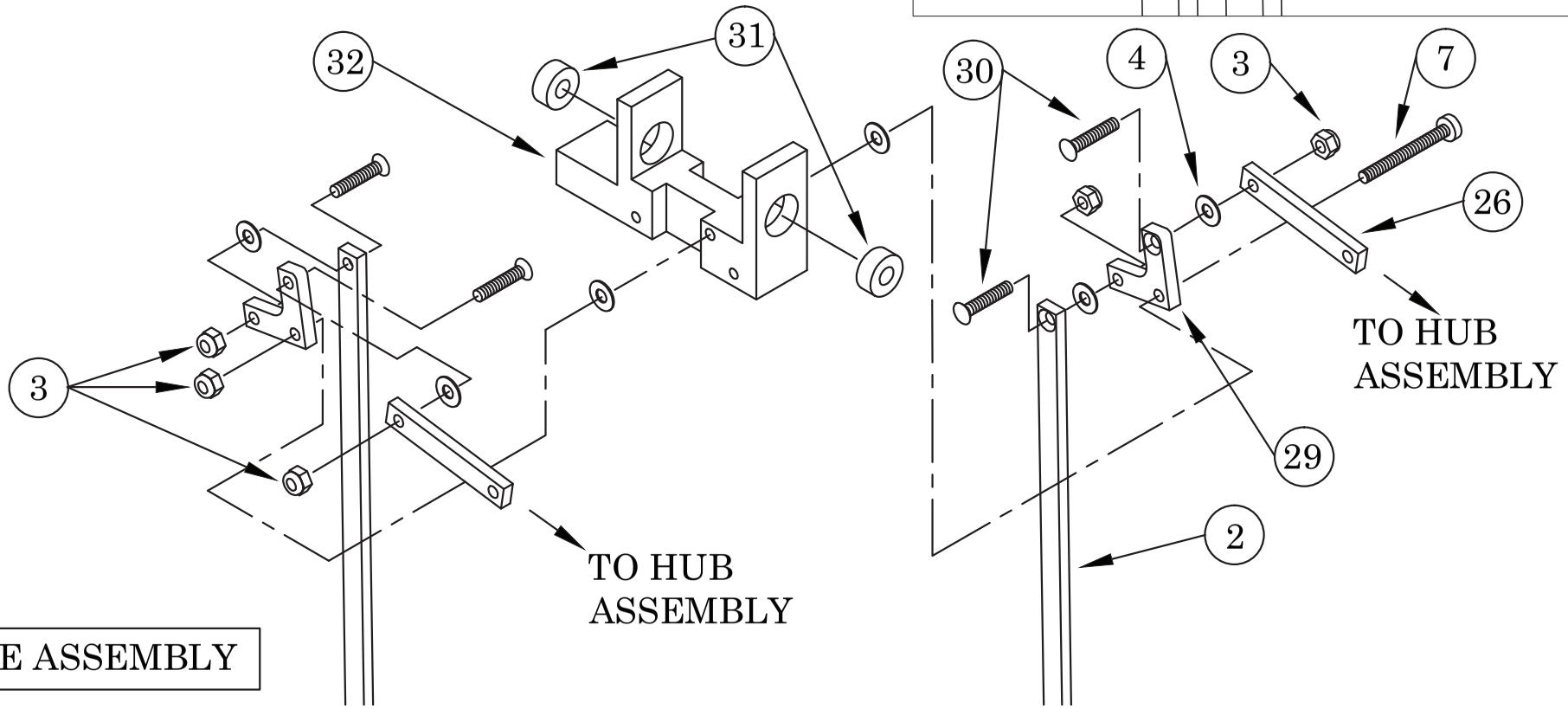

FRAME ASSEMBLY

ITEM	QTY	NAME	MATERIAL
12	4	M2x0.4 3mm SET SCREW	STEEL
33	1	POLYCARBONATE LID	POLYCARBONATE
34	1	MEDICAL TUBING	RUBBER
35	1	1/8" CUBE MAGNET	NEODYMIUM
36	2	TOWER	ALUMINUM
37	2	1/4"-20 1" SOCKET HEAD CAP SCREW	STEEL
38	2	4-40 3/16" SOCKET HEAD CAP SCREW	STEEL
39	2	4-40 3/16 SHCS COVER	NYLON

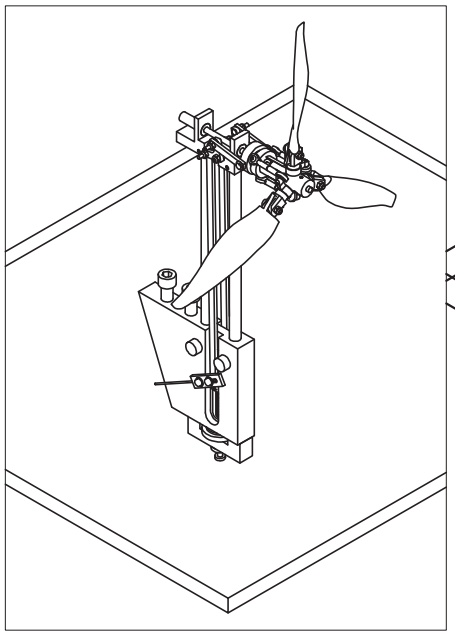

WIND TURBINE